Link Budget Analysis for cmWave Communication Between LEO Satellites and Handheld User Equipment

Master's thesis in Information and Communication Technology

JAHANVI BHADRASHETTY DINESH

Department of Electrical Engineering
CHALMERS UNIVERSITY OF TECHNOLOGY
Gothenburg, Sweden 2025

Master's thesis 2025

Link Budget Analysis for cmWave Communication Between LEO Satellites and Handheld User Equipment

A Master of Science thesis in the Information and Communication Technology Master's Programme

JAHANVI BHADRASHETTY DINESH

Department of Electrical Engineering
Division of Communications, Antennas and Optical Networks (CAOS)
Chalmers University of Technology
Gothenburg, Sweden 2025

Link Budget Analysis for cmWave
Communication Between LEO Satellites and Handheld User Equipment
A Master of Science thesis in the Information and Communication Technology Master's Programme (MPICT)
Jahanvi Bhadrashetty Dinesh

Supervisor: Gang Zou, Henric Broström, Giuseppe Moschetti, Ericsson AB, Charitha Madapatha and Tommy Svensson, Chalmers
Examiner: Tommy Svensson, Department of Electrical Engineering

Master's Thesis 2025
Division of Communications, Antennas and Optical Networks (CAOS), Department of Electrical Engineering
Chalmers University of Technology
SE-412 96 Gothenburg
Telephone +46 31 772 1000

Typeset in LaTeX
Gothenburg, Sweden 2025

Link Budget Analysis for cmWave
Communication Between LEO Satellites and Handheld User Equipment
Jahanvi Bhadrashetty Dinesh
Department of Electrical Engineering
Chalmers University of Technology

Abstract

This master thesis report explores the viability and performance of Distributed Multiple-Input Multiple-Output (D-MIMO) systems in Low Earth Orbit (LEO) satellite constellations for a handheld user equipment (UE). A MATLAB-based link budget framework is developed to simulate the uplink and downlink scenarios between the satellites and the UE, while considering different elevation angles.
Realistic assumptions from various 3rd Generation Partnership Project (3GPP) and International Telecommunications Union(ITU) standards, including those for atmospheric and rain attenuation have been used. Asymmetric power allocation procedures have been explored to optimize the reliability of the link as well as spectral efficiency. This model dynamically calculates bit error rate (BER) and signal-to-noise ratio (SNR) among others. Important parameters like Doppler shift and propagation delay are examined to assess their impact on the throughput and robustness of D-MIMO.
The simulation results demonstrate that intelligent resource allocation across multiple satellites and antennas can significantly enhance the achievable data rate and reliability for next-generation satellite communication systems.

Keywords: D-MIMO, LEO satellite communication, Link Budget Analysis, Uplink and Downlink Modelling, Signal-to-noise Ratio(SNR), Spectral Efficiency, MATLAB Simulation.

Acknowledgements

Firstly, I'd like to thank my manager Rickard Ljung and supervisor Gang Zou for believing in my abilities from early on and giving me a free reign to independently drive this project. Also, a huge thanks to my supervisors from Chalmers, Charitha Madapatha and Tommy Svensson(examiner) for their guidance over the last 6 months. This project could not have been completed without your expertise and support.

Next, I'd like to thank my parents Prathima and Dinesh, and my brother Aditya for providing unwavering uplink support throughout this journey and spending countless days and nights reassuring and motivating me — even when I felt like I was out of coverage.

Lastly, I'd like to thank my friends Ana, Yusheng, Advait and Pratheek for always believing in me. You all acted as my ground station at various moments in the last 2 years, keeping me connected and stable and I could not have done this without your encouragement.

Jahanvi Bhadrashetty Dinesh, Gothenburg, July 2025

To my dear appaji, who helped me dream but couldn't be here to see me live it.

List of Acronyms

3GPP	3rd Generation Partnership Project
5G and 6G	5th Generation and 6th Generation
AWGN	Additive White Gaussian Noise
BER	Bit Error Rate
CNR	Carrier-to-Noise Ratio
C/No	Carrier-to-Noise Density Ratio
CSI	Channel State Information
D-MIMO	Distributed Multiple-Input Multiple-Output
D2C	Direct-to-Cell
DL	Downlink
Eb/No	Energy per bit to Noise Power Density Ratio
ECEF	Earth-Centered, Earth-Fixed
EIRP	Effective Isotropic Radiated Power
FSS	Fixed Satellite Service
FSPL	Free Space Path Loss
G/T	Figure of Merit (Gain-to-Temperature ratio)
GEO	Geostationary Earth Orbit
GPS	Global Positioning System
HAPs	High-Altitude Platforms
IoT	Internet Of Things
ISL	Inter-Satellite Links
ITU-R	International Telecommunications Union - Radio-communications sector
LEO	Low Earth Orbit
LoS	Line of Sight
MEO	Medium Earth Orbit
MIMO	Multiple-Input Multiple-Output
MNO	Mobile Network Operators
MSS	Mobile Satellite Service
NTN	Non-Terrestrial Networks
QAM	Quadrature Amplitude Modulation
QoS	Quality of Service
QPSK	Quadrature Phase Shift Keying
RF	Radio Frequency
SNR	Signal-to-Noise Ratio
UAVs	Unmanned Aerial Vehicles
UE	User Equipment
UL	Uplink
VSAT	Very Small Aperture Terminal

Nomenclature

Below is the nomenclature of indices, parameters, and variables that have been used throughout this thesis.

Indices

ant	Antenna
At	Atmosphere
$down$	Downlink
o	Dry air
R	Rain
RX	Receiver
sat	Satellite
sys	System
TX	Transmitter
UE	User equipment
up	Uplink
w	Water vapour

Parameters

A_{sat}	Satellite antenna aperture (unitless)
A_{UE}	UE antenna area (m^2)
B	System bandwidth (Hz)
c	Speed of light (m/s)
F	Noise factor (linear)
G_R	Receiving antenna gain (dBi)
G_T	Transmitting antenna gain (dBi)
G/T	Figure of merit (dB/K)
$g_{UE,1}$	Gain per UE antenna element (dB)
h_{sat}	Satellite altitude (m)
h_r	Rain height (km)
h_0	Isotherm height above mean sea level (km)
k	Boltzmann constant (J/K)
M	Modulation order

$N_{UE,ant}$	Number of UE antenna elements
NF	Noise figure (dB)
R_b	Bit rate (bps)
R_E	Earth radius (m)
R_r	Rain rate (mm/h)
T_A	Antenna noise temperature (K)
$T_{e,RX}$	Receiver noise temperature (K)
T_{rec}	Receiver noise temperature (K)
T_{sys}	System noise temperature (K)
T_0	Reference temperature (K)
α	Polarization coefficient
η	Antenna efficiency
θ_{3dB}	Half power beam width (degrees)
θ_r	Antenna pointing error (degrees)

Variables

C	Carrier Power(dBW)
N_0	Noise Power Spectral Density (dBW/Hz)
d	Distance between satellite and UE (m)
E_b/N_0	Energy per bit to noise power density ratio (dB)
f	Carrier frequency (Hz)
f_D	Doppler shift frequency (Hz)
f_{down}	Downlink frequency (Hz)
f_{up}	Uplink frequency (Hz)
L_A	Atmospheric attenuation (dB)
L_{ap}	Antenna pointing loss (dB)
L_{At}	Atmospheric loss (dB)
L_f	Feeder loss (dB)
L_M	Miscellaneous losses (dB)
L_O	Other losses (dB)
L_P	Free space path loss (dB)
L_p	Polarization loss (dB)
L_R	Rain loss (dB)
P_R	Received power (dBW)
P_T	Transmitted power (dBW)
r	Satellite orbital radius (m)
v_{rel}	Relative velocity (m/s)
v_r	Radial velocity component (m/s)
x_s, y_s, z_s	Satellite ECEF coordinates (m)
x_u, y_u, z_u	UE ECEF coordinates (m)
γ	Specific attenuation (dB/km)
γ_o	Specific attenuation of dry air (dB/km)
γ_R	Specific attenuation due to rain (dB/km)
γ_w	Specific attenuation of water vapour (dB/km)

θ	Elevation angle (degrees)
λ	Wavelength (m)
λ_{down}	Downlink wavelength (m)
λ_{up}	Uplink wavelength (m)
ϕ_s	Satellite latitude (degrees)
ϕ_u	UE latitude (degrees)
τ	Propagation delay (s)

Contents

List of Figures

List of Tables

1

Introduction

1.1 Background

Over the last decade, the number of smart devices has grown exponentially which have various Quality of Service (QoS) requirements. Although this represents a significant leap in connectivity and technology, it also creates a demand for ubiquitous connectivity, posing significant challenges for terrestrial networks. According to the Ericsson Mobility Report [1], there will be approximately 3.3 billion 5G users by the end of 2027. As the number of users increases, terrestrial networks cannot provide fully wireless communication coverage of all sensors and devices, which may lead to service interruptions. It is becoming a challenge to ensure high-quality service for users, regardless of whether they are in a dense urban city, a remote forest, or traveling on a cruise ship or airplane.

Since the early 1990s, terrestrial communication has revolutionized mobile connectivity, creating a boom in the telecommunications industry. During the same time, satellite communications also gained traction, with companies such as Inmarsat and Iridium pioneering geostationary earth orbit (GEO) and low earth orbit (LEO) satellites. However, these companies struggled to compete with terrestrial mobile networks, which expanded rapidly due to their lower cost and ease of deployment. In the early 2010s, satellite mobile systems experienced a resurgence with the deployment of massive LEO constellations aimed at delivering high-speed internet for both terrestrial and satellite systems.

Terrestrial networks, while only covering 6% of the Earth's surface, provides high data rates and low latency [2]. However satellite mobile systems provide truly global coverage and are more resilient to natural disasters or technical failures that commonly affect terrestrial infrastructure. To address these limitations, 5th generation (5G) networks have increasingly integrated terrestrial and satellite communications to ensure seamless, uninterrupted connectivity worldwide. As the world now prepares for the release of 6G, satellite communications will play an even larger role in expanding global coverage and reliability.

The International Telecommunications Union (ITU) is the global agency responsible for facilitating communication by allocating radio spectrum and establishing standards to ensure smooth connectivity. In collaboration with the 3rd Generation Partnership Project (3GPP), ITU releases technical reports that outline current research and technological advancements. One such report, 3GPP TR 38.811 [3] from Release 15, introduced the integration of terrestrial and non-terrestrial networks as

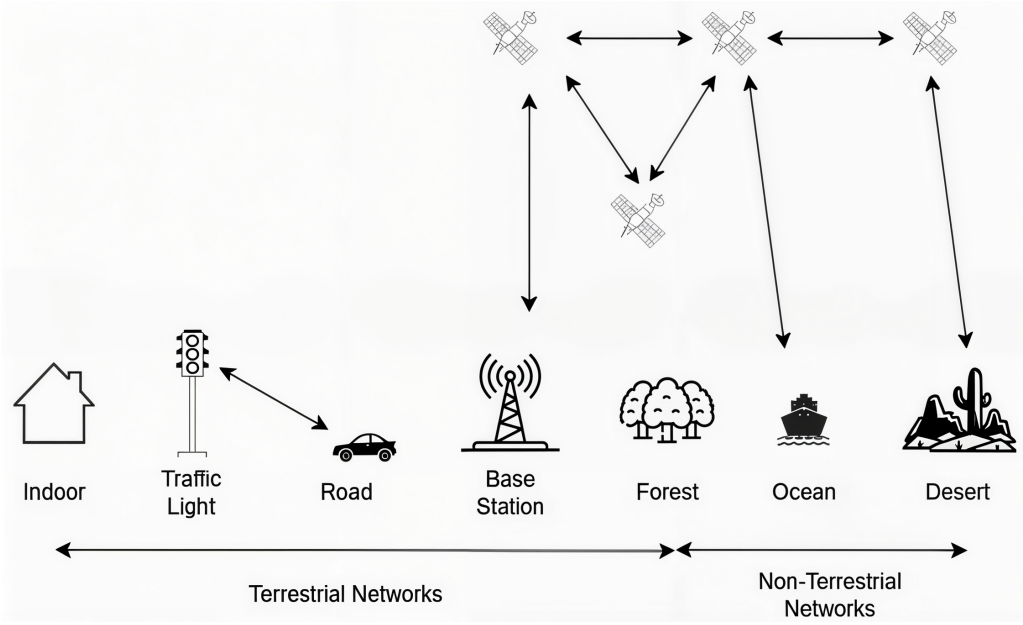

Figure 1.1: Terrestrial and non Terrestrial Networks

seen in Figure 1.1. This has been done considering S-band (used by Inmarsat) and Ka-band (used by Starlink) due to higher data rates, long-range connectivity, and better resistance to weather conditions.

Historically, Ku-band has not been the preferred choice for satellite communications because of its lower bandwidth and data rates, which can result in higher operational costs. Furthermore, it requires larger antennas and is more susceptible to adverse weather conditions. However, its well-established infrastructure allows for cost-effective deployment, making it a viable option for certain applications. Additionally, Ku-band strikes a balance between antenna size and performance, making it suitable for remote VSAT terminals, direct-to-cell applications, and weather-resistant communication systems. In parallel, X-band offers enhanced reliability and resistance to weather-related disruptions, making it ideal for secure and mission-critical satellite communications. Based on these advantages, this study will assess the viability of integrating the Ku-band and X-band for satellite communications, by performing a link budget analysis.

1.2 Purpose and Goal

This work will focus on analyzing the uplink and downlink link budget between a satellite and a mobile hand-set terminal.

While traditional communication networks have worked well for decades, users' needs are rapidly changing, and there is a huge focus on always being online. This can be in the form of Internet of Things (IoT) devices or just being able to make phone calls while in out-of-service regions such as forests. This was the starting point for the boom of direct-to-cell (D2C) services which enable a person to do just about anything from sending basic text messages to browsing the internet. D2C is

a relatively new technology in which a cellphone (or any 3GPP compatible device) communicates directly to a satellite, eliminating the need for a ground station and setup. This can be implemented in 2 ways:

- Satellite network operators (SNO) like Starlink and mobile network operators (MNO) such as T-mobile collaborate to allow this service to be carried out on the MNOs licensed radio spectrum. In essence, the satellite is developed and deployed to work with the UE.
- The device is equipped with a small chip that enables it to "talk" to a specific satellite. This is observed in the partnership between Globalstar and Apple [4].

D2C services have many advantages such as- real global connectivity, reliable communication for first responders or users during a natural disaster or emergency situation, as well as the general public while traveling through otherwise unreachable areas such as deserts or cruises.

Since 2024, Starlink has partnered with T-Mobile and OneNZ to provide D2C service (Figure 1.2) to users in the United States of America (USA) and New Zealand. The purpose of this service is to provide ubiquitous coverage even in dead zones of terrestrial networks. They launched more than 400 satellites that act as cell towers in space to increase coverage to almost every corner of the world [5]. These are LEO satellites that fly a few hundred kilometers above the Earth at very high speeds. While this provides great coverage, low latency, and high data-rates, this setup needs a lot of considerations such as RF carrier frequency, bandwidth, data-rates needed, antenna parameters and weather resilience before deployment.

In order to design and access such a setup and look into the previously mentioned considerations, a link budget calculation is needed. This link budget will help link the requirements of the system with the expected results.

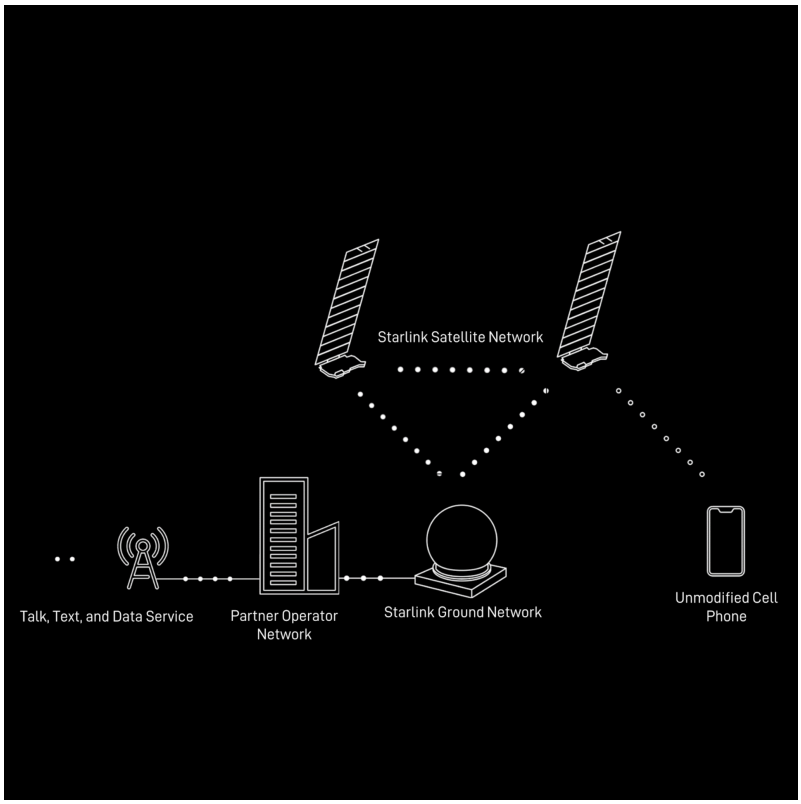

Figure 1.2: Starlink satellite network visualization [18].

2

Technical Background

2.1 Non Terrestrial Networks

Non-Terrestrial networks (NTN) are communication networks that function above the surface of the Earth, with the help of satellites, high-altitude platforms (HAPs) and unmanned aerial vehicles (UAVs). These NTNs help to enable connectivity in remote, under-served or inaccessible regions of terrestrial networks. They help bridge the gap between terrestrial networks and obtaining truly ubiquitous connectivity. This is done by integrating NTNs into 5G and future 6G system architectures to support various services such as emergency communications, broadband internet and IoT connectivity [5].

NTNs are divided into three categories as can be seen in Figure 2.1: satellite systems, HAPs and UAVs. HAPs operate at an altitude of about 20 km above the Earth and consist of platforms such as hot-air balloons (e.g. Loon) and solar powered aircrafts such as Airbus Zephyr. These provide connectivity in smaller regions. UAVs, fly at about 5 km altitude and are usually mainly used for emergency services and disaster relief applications [6].

This work focuses on satellite systems. Satellite systems are further classified (based on their orbits) as - LEO, Medium Earth Orbit (MEO), GEO. Each of these have unique tradeoffs in terms of orbital time, coverage, latency and use cases. LEO constellations such as Starlink and Iridium provide high throughput of data with low latency because of their altitudes. However, GEO satellites such as Inmarsat, orbiting the Earth at a much higher altitude provide a larger area of coverage [2].

NTNs are experiencing their second wave of popularity through companies such as Starlink, Applications Technology Satellite (ATS) and Globalstar. 3GPP in Release 17 of the 5G standardization documentation included NTN services. This in turn initiated what is today called the 'Space Race' [7].

Therefore, this chapter provides an insight into the basic technical foundation needed to understand the operation and integration of NTNs with existing networks. The upcoming sections will explore satellite-based NTN architectures, link budget parameters, radio signal propagation losses and integration methods.

2.1.1 Satellite Communications

Satellite communications are an important part of NTNs, providing global coverage and infrastructure for communication for many different applications. The main

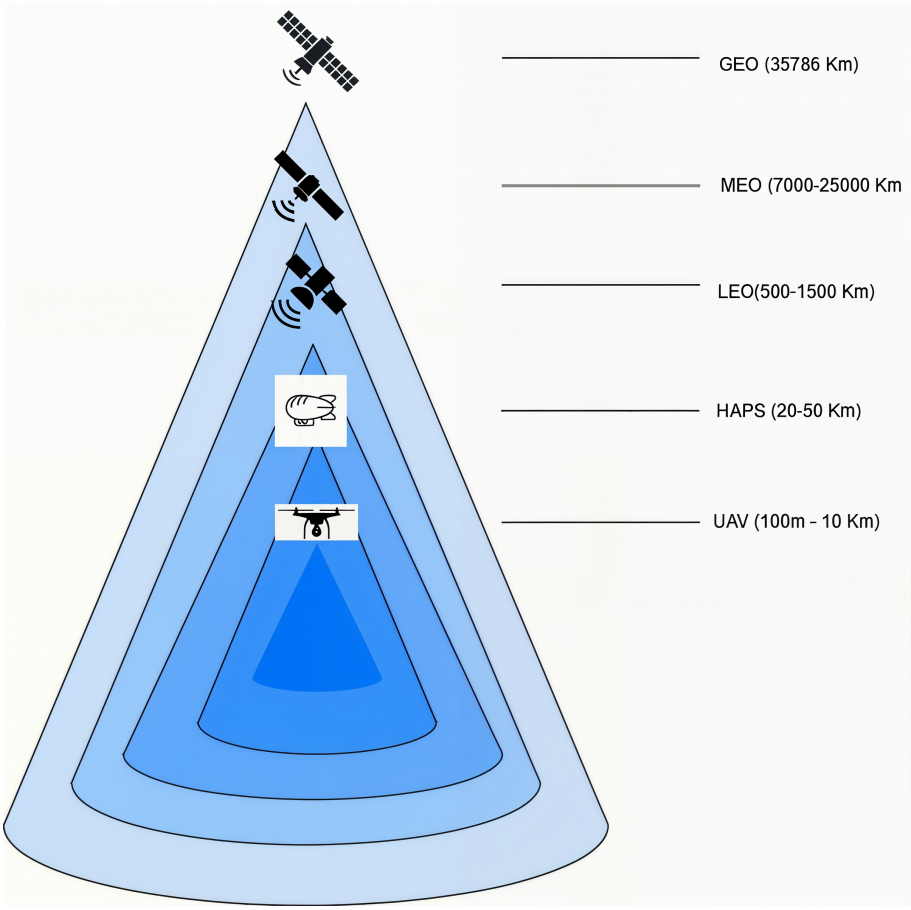

Figure 2.1: Types of Non-Terrestrial Networks

advantage of satellite Communications is the ability to have long-distance line-of-sight communications from almost anywhere in the world. Table 2.1 describes the different categories of satellites and their properties.

Parameter	LEO	MEO	GEO
Altitude Range (km)	500–2,000	2,000–20,000	35,786
Orbital Period	90–120 min	2–12 hrs	24 hrs
Coverage Area	Small (regional)	Medium (continental)	Large (global at equator)
Latency (one-way)	5–25 ms	50–150 ms	250–300 ms
Doppler Shift	High	Moderate	Low
Number of Satellites Required	Dozens to hundreds	Dozens	3 for global (at equator)
Launch	Lower cost, frequent	Moderate cost	High cost
Use Cases	IoT, low-latency comms, Earth observation	GNSS (e.g., GPS), data relay	TV, broadband, weather, backhaul
Ground Tracking Complexity	High	Moderate	Low (stationary from Earth)
Mobility Support	Strong (fast handovers)	Moderate	Weak

Table 2.1: Comparison of LEO, MEO, and GEO Satellite Orbits [12]

The evolution of satellite communication is driven by major advancements in satellite systems, beamforming techniques and the use of artificial intelligence in mobility management. These improvements help to increase overall throughput, minimize latency and ensure efficient usage of available spectrum. Satellites are also being used in combination to form hybrid constellations to dynamically allocate resources based on capacity and user location.

The integration of satellite communications with 5G and 6G is the driving force

behind the use of space-based technology in combination with existing networks. Standardization initiatives by 3GPP and ITU have further helped pave the way for a truly global and resilient communication system [8].

2.1.2 LEO Constellations and Architecture

LEO satellites are currently popularly used in satellite communication practices especially with respect to NTN and 5G/6G standards. Although GEO/MEO satellites have better coverage than LEO satellites, they have much higher latency. Since LEO satellites are at a lower altitude, they have lower latency and they travel at very high velocity. These high velocities also create huge Doppler effects that need to be considered while simulating LEO satellites. All of these factors are considered in the modeling and simulation discussed in this thesis.

2.1.2.1 Orbital characteristics

LEO satellites orbit the Earth at altitudes ranging from 500 to 2000 kilometers above its surface. Due to their low altitudes, they have an orbital time of about 90-120 minutes, at a velocity of about 7.8 km/s. This high velocity leads to Doppler shift and fast varying link characteristics which need to be considered during link budget calculations.

2.1.2.2 Constellation Design

LEO satellites, unlike GEO, do not remain fixed relative to a ground user. They need constellations made up of multiple satellites which work together to optimize coverage and ensure smooth handovers.

This thesis uses 3 types of LEO satellite constellations in increasing order of complexity, as depicted in Figures 3.2, 3.3 and 3.4 in the upcoming sections. They enable a detailed analysis of link budget parameters, Doppler effects, and signal path characteristics.

2.1.2.3 Relevance to Link budget and Doppler mapping

LEO constellations uniquely affect link budget calculations as indicated below:

- Shorter slant ranges reduce the free-space path loss, improving the received power.
- Low elevation angles result in increased path losses and greater atmospheric attenuation.
- High orbital speed introduces large Doppler shifts, requiring Doppler-aware link design.
- Frequent beam transitions can lead to fast channel variation, affecting coherence time and synchronization.

Understanding these characteristics is critical for accurately modeling MIMO satellite links, per-path Doppler spread, and adaptive modulation performance, as carried out in later chapters of this thesis.

2.2 Fundamentals of Link Budget Analysis

2.2.1 Definition and Importance of Link Budget

A link budget is a set of equations used to account for all the gains and losses experienced by a signal as it propagates between a satellite and an UE. It predicts the approximate power received based on different parameters such as signal frequency, transmission power, antenna gains, losses due to various factors, and noise. Essentially, it is a power balance sheet that predicts whether the communication system is feasible or not. Mathematically, a link budget can be expressed in dB as

$$P_{Rx} = P_{Tx} + G_{Tx} + G_{Rx} - L_P - L_A - L_O. \tag{2.1}$$

Here,

- P_{Rx} = Received Power
- P_{Tx} = Transmitted Power
- G_{Tx} = Gain of transmitting antenna
- G_{Rx} = Gain of receiving antenna
- L_{P} = Free space path loss
- L_{A} = Atmospheric attenuation
- L_{O} = Other Miscellaneous losses

In satellite communications, specifically on LEO based systems, the satellites experience high speeds, rapid changes in elevation angles and slant range as well as Doppler shift. Therefore, having such a tool ensures that the communication link meets the requirements while preventing oversizing transmission power and antennas, thus optimizing cost and energy. Link budgets also incorporate delay spread, Doppler shifts, and different propagation models which are different compared to those in a terrestrial system. They help model the entire ecosystem before deployment, which gives a better picture of various parameters.

2.2.2 Components of a Link Budget

A link budget emulates all the losses and gains which, when combined represent the strength of the signal transmitted and received. Each component has effect on the overall power received and also on the strength and quality of the link. LEO satellite systems function in an ever-changing conditions such as constantly varying slant distances, elevation angles, and atmospheric effects. Therefore, the link budget is used to ensure reliable communication through system optimization.

2.2.2.1 Transmit Power (P_{Tx})

The power transmitted (P_{Tx}) is the power of the signal delivered from a transmitter to its antenna port. This transmitter could be part of a satellite, base station or ground hub. P_{Tx} usually has a huge effect on the link budget and is considerably

high to account for path loss and atmospheric attenuation. The power transmitted depends on regulatory restrictions, limitations of the satellite / UE platform, and the required data ranges.

2.2.2.2 Transmit Antenna Gain (G_{Tx})

Antenna gain indicates the ability of the antenna to direct the signal energy (beam) in a particular direction. Therefore, G_{Tx} is the gain on the transmitter side of the system. In LEO systems, electronically steerable phased array antennas are usually used to dynamically adjust the beam direction and maintain links without interruption in communication. The value of this gain depends on the design of the antenna and the operating frequency.

2.2.2.3 Receiving Antenna Gain (G_{Rx})

The receiving antenna's ability to efficiently collect the signal from the transmitter is indicated by its gain. Antennas on the ground can be fixed or electronically steerable, but mobile UEs use phased array or patch antennas.

2.2.2.4 Free Space Path Loss (L_{P})

Free space path loss indicates the loss in signal strength due to the attenuation of the signal over a certain distance. It depends on distance between the transmitter and the receiver and the operating frequency. In LEO satellites, the distance changes constantly because the satellites are moving fast in orbits above Earth, so the value of L_{P} also changes constantly.

2.2.2.5 Atmospheric and Propagation Losses (L_{A})

Signals in both uplink and downlink pass through the atmospheric and are effected by absorption due atmospheric gases, water vapour and weather conditions. As the frequency of the signal increases, the effect of these losses also increases. When considering LEO satellites, in which elevation angles change constantly, atmospheric losses also vary accordingly. These losses can be predicted using empirical models set by the International Telecommunications Union - Radio-communications sector [9] [10].

2.2.2.6 Other Losses (L_{O})

Additionally, the signal is susceptible to losses due to polarization mismatch, antenna pointing mismatch, hardware imperfections and transmission line attenuation. Since LEO satellites have fast orbital movement, these losses are unavoidable and any deviation from the optimal antenna pointing leads to reduction in gain and increases in losses. Therefore, these losses need to be considered to avoid overestimating the performance of the link.

2.2.2.7 Figure of Merit (G/T)

Along with the power received, the G/T ratio is often used to reflect the RF receiver's ability to receive and process weak signals in a noisy background. This ratio is highly susceptible to environmental factors, antenna design characteristics, and the circuit design of the receiver such as low noise amplifiers and filters used.

2.3 Factors affecting Link Budget Performance

The performance of a satellite communication link, specifically a LEO satellite is very sensitive to dynamic environmental and system-level factors. Since LEO satellites are in constant motion with respect to the Earth, the communication link has different conditions at different instances of time. Therefore, a robust link budget analysis should not only take into consideration the main link but also the factors that affect the total strength of the signal [11].

2.3.1 Elevation Angle and Slant Range

Elevation angle is defined as the angle between the satellite and the horizon at the UE (as depicted in Figure 2.2). It directly effects the slant range, free space path loss and atmospheric attenuation. The elevation angle is inversely proportional to the slant range. As elevation angle decreases, the path loss increases significantly along with greater atmospheric attenuation because the signal will now have to travel a longer distance through the atmosphere to get to the receiver. Traditional link budget models usually rely on best and worst case assumptions of elevation angles. However, statistical models capture its probabilistic behavior and provide a better picture of the expected signal strength [5].

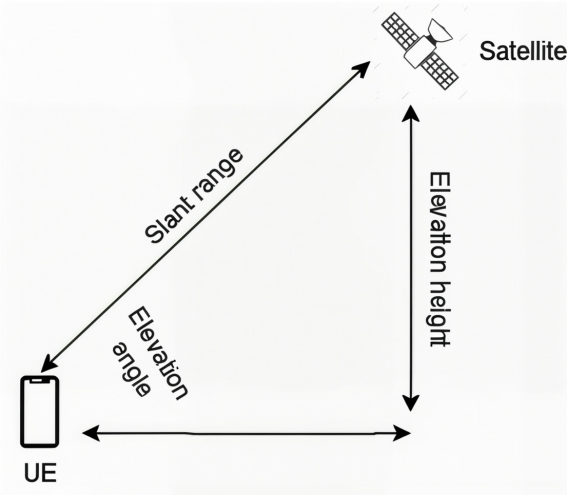

Figure 2.2: Elevation angle and slant range

2.3.2 Doppler shift and frequency stability

While transmitting RF signals, LEO satellites move at a speed of about 7.8 km/s with respect to the Earth, which in turn produces significant Doppler shifts on the RF signal received by a device on the Earth [12]. This causes the frequency of the received signal to change over time, making it necessary for the receiver to perform carrier frequency synchronization in order to correctly demodulate the signal and therefore increasing complexity of signal processing. The magnitude of the Doppler shift is influenced by the satellite's velocity and elevation angle, with the highest shifts occurring when the satellite is near the horizon [13].

2.3.3 Interference and Frequency Sharing

As the spectrum becomes more congested, LEO satellites are now sharing frequencies with terrestrial services or other satellites. This could lead to interference in adjacent beams or even satellites/ UEs close to each other. Then, interference management becomes an important consideration while integrating it with terrestrial networks where frequency reuse outside cells, beamforming and other protocols need to be implemented to ensure secure communication [14].

2.3.4 Environmental and Ionospheric Effects

Environmental factors such as Faraday rotation and ionospheric scintillation play a role in link degradation. Scintillation causes massive fluctuations in the amplitude and phase but Faraday rotation only affects the polarization of the signal. These effects are heightened during solar activity like solar flares because the ionospheric density is elevated.

2.3.5 System Hardware Limitations

The performance of a satellite link also depends on hardware limitations on the UE or the satellite side. This could be limitations in transmitter power, antenna gains, efficiency of low noise amplifiers and temperature of various components. There could also be losses between the components within a system and losses due to cables, feeders and connectors that add on to the overall degradation of signal strength.

2.4 Mathematical Framework of link budget

The link budget as mentioned earlier can be expressed as a series of mathematical relationships that indicate the power received over a link. These formulas are foundational in satellite system design and are used in performance validation as well as regulatory filings for satellites, standardization documents to ensure interoperability and performance compliance across NTN systems.

2.4.1 Received Power (P_{Rx})

This is the main equation used to calculate the link budget. It has been discussed in equation 2.1 of subsection 2.2.1:

2.4.2 Free Space Path Loss (L_{P})

L_{P} (dB) describes signal attenuation due to propagation and is given by equation

$$L_P = 20\log_{10}(d) + 20\log_{10}(f) + 20\log_{10}\left(\frac{4\pi}{c}\right), \tag{2.2}$$

where,

- d = LoS distance between the transmitter and receiver (m),
- f = Carrier frequency (Hz),
- c = speed of light (m/s).

This equation is valid for Line of Sight(LoS) propagation without additional obstructions and is critical in LEO systems where slant range(d) changes constantly due to motion of the satellite.

2.4.3 Effective Isotropic Radiated Power (EIRP)

EIRP is a measure of output power radiated from an isotropic antenna in a particular direction. It is also mathematically described as the maximum power emitted by the antenna in the direction with the highest antenna gain. $EIRP$ expressed in dBW is denoted by equation

$$EIRP = P_{\mathrm{Tx}} + G_{\mathrm{A}}. \tag{2.3}$$

Here,

- P_{Tx} = Output power transmitted (dBW),
- G_{A} = Antenna gain (dBi).

2.4.4 Doppler shift and Propagation Delay

Doppler shift between the UE and LEO satellite is denoted by equation f_{d} (m/s/Hz) in

$$f_d = \frac{v_r f}{c}. \tag{2.4}$$

Here,

- v_r = relative velocity between the satellite and the UE (m/s),
- f = frequency of the signal transferred between the UE and LEO satellite (Hz).

Propagation Delay (τ (s)) is given by equation

$$\tau = \frac{d}{c}, \tag{2.5}$$

where d is the distance between the satellite and UE (m).

2.4.5 Other Losses (L_{O})

2.4.5.1 Polarization Loss L_{P}

Polarization loss is the power loss due to the polarization mismatch between transmitter and receiver antennas, which can lead to signal degradation. In satellite communication applications, circular polarization is usually preferred because it counters multi-path effects and is less affected by atmospheric conditions. This kind of loss is quantified using equation

$$L_p = -10 \log_{10} \left(\cos^2 \theta \right), \tag{2.6}$$

where θ is the angle between the polarization vectors of the transmitting and receiving antennas (degrees).

In this thesis, circular polarization is assumed on both the transmitter and receiver side. Therefore polarization loss can be neglected.

2.4.5.2 Antenna pointing loss L_{ap}

Antenna pointing Loss is the reduction in signal strength due to misalignment of antenna directivity on either the transmitter side, the receiver side or both. Correct alignment between the UE and the satellite provides maximum gain. Antenna pointing loss is given by equation

$$L_{ap} = 12 \left(\frac{\theta_r}{\theta_{3db}} \right)^2, \tag{2.7}$$

where,

- θ_r = antenna pointing error (degrees),
- θ_{3dB} = Half Power Beam Width (HPBW).

In this thesis, antenna pointing loss is assumed to be 0.25 dB.

2.4.5.3 Atmospheric loss L_{At}

Atmospheric loss can be calculated from ITU - Radio recommendation P.676.12 [10]. Equation 1 in [15] can be simplified as equation

$$\gamma = \gamma_o + \gamma_w. \tag{2.8}$$

Here,

- γ_{o} = Specific attenuation of dry air,
- γ_{w} = specific attenuation of water vapour.

The value of γ_{o} can be calculated using equation

$$\gamma = kR_r^{\alpha}. \tag{2.9}$$

Here,

- γ_{R} = specific attenuation (dB/km),
- R_{r} = rain rate (mm/h),
- k = frequency coefficient,
- α = polarization coefficient.

However, in this thesis, The value of L_{At} is calculated directly by plugging in the values of γ_o and γ_w taken from Figure 1 of [15].

2.4.5.4 Rain loss (L_{R})

Loss due to rain is calculated using ITU Radio recommendation P.838-3 [9]. Figure 1 from ITU-R P.837 [15] is used to calculate Rain rate (R_{R}). Then equation 2.9 is used to calculate the specific attenuation due to rain. Next, equation 2.10 from ITU-R P.839-4 [17] is used to calculate the rain height model h_r.

$$h_r = h_o + 0.36, \tag{2.10}$$

where h_o is the isotherm height above mean sea level (m).

Lastly, the final rain loss (L_{R}) in dB is calculated using equation

$$L_{\mathrm{R}} = h_{\mathrm{R}} + \gamma_{\mathrm{R}}. \tag{2.11}$$

2.4.6 System Noise Temperature and Figure of Merit

The figure of merit of a receiver is expressed by as

$$\frac{G}{T} = G_{\mathrm{Rx}} - 10\log_{10}(T_{\mathrm{sys}}). \tag{2.12}$$

T_{sys} stands for System Noise Temperature (K) and it is a measure of the total noise power introduced by the receiving system including antenna, cables, low noise amplifier, receiver. Mathematically,

$$T_{\mathrm{sys}} = T_{\mathrm{ant}} + T_{\mathrm{Rx}}, \tag{2.13}$$

where,

- T_{ant} = Noise temperature from the antenna (sky, ground, sun),
- T_{Rx} = Noise on the receiver side (from low noise amplifier, mixer and cables).

A higher G/T ratio indicates better receiver performance. This is also used to calculate the carrier-to-noise ratio (C/N) and link margin.

2.4.7 Carrier-to-noise Density Ratio (C/N_0)

C/N_0 is the most popular parameter used to evaluate the quality of the incoming signal. It is indicated by equation

$$\frac{C}{N_0} = \text{EIRP} + G_{\text{Rx}} - L_{\text{P}} + L_{\text{At}} - L_{\text{O}} - 10\log_{10}(kT_{\text{s}}), \tag{2.14}$$

where k is the Boltzmann's constant (-228.6 dBWs/K/Hz) and T_{sys} is the System noise temperature (K).

2.4.8 Energy per bit to Noise Power Density (E_b/N_0)

E_b/N_0 is a ratio used when assessing whether a particular modulation technique can function within the predicted link conditions.

$$\frac{E_{\text{b}}}{N_0} = \frac{C}{N_0} - 10\log_{10}(R_{\text{b}}), \tag{2.15}$$

where R_{b} is the bit rate (bps) and C/N_0 is the Carrier-to-noise Density Ratio (dBHz).

2.4.9 Adaptive Modulation and throughput metrics

Current satellite communication systems function in very dynamic environments where channel parameters vary due to slight changes in elevation angle, atmospheric losses, and frequency shifts. To optimize spectral efficiency usage while maintaining a reliable link, adaptive modulation is used. This technique adjusts modulation schemes on the fly, based on the instantaneous channel quality.

2.4.9.1 Modulation vs spectral efficiency

Different modulation formats offer different trade-offs between robustness and spectral efficiency. The following modulation schemes are widely used in satellite communications:

- Binary Phase Shift Keying (BPSK): Highly robust; 1 bps/Hz
- Quadrature Phase Shift Keying (QPSK): Balanced; 2 bps/Hz
- 16-Quadrature Amplitude Modulation (16-QAM): Higher throughput; 4 bps/Hz

The theoretical efficiency η (bps/M) is

$$\eta = \log_2(M), \tag{2.16}$$

where M is the modulation order. However, the actual efficiency depends on the Eb/N0 values.

2.4.9.2 Adaptive Modulation and (E_b/N_0)

In the simulation model presented in this thesis, the modulation order is dynamically selected based on the calculated E_b/N_0 values. The following thresholds are used as part of the adaptation logic:

- If $E_b/N_0 <$ 3dB : BPSK ($\eta = 1$)
- If 3 <= E_b/N_0 <= 6 dB : QPSK ($\eta = 2$)
- If E_b/N_0 >= 6dB : 16 QAM ($\eta = 4$)

These thresholds allow the system to maximize the data rate while maintaining a reliable link under varying satellite-UE conditions.

3

Methods

3.1 Introduction to methodology

This chapter details the methodology followed to analyze and evaluate the performance of LEO satellite communication links. The goal is to develop a reliable link budget framework that considers the physical layer characteristics of an NTN.The approach integrates modeling the channel from a theoretical perspective including standardized models to predict RF signal losses, to estimate the received power under different conditions.

3.2 System architecture and design

This section outlines the architectural and design considerations of the LEO satellite communication system modeled in this study. It focuses on the end-to-end communication link between a LEO satellite and a handheld UE, capturing the unique challenges posed by mobility, hardware limitations, and dynamic link conditions. The objective is to define the operating parameters of the physical layer structure and the operational parameters that influence the link budget and overall system performance.

The subsections cover the technical configuration of the user terminal and satellite, the rationale behind the selection of operating frequency bands, and a set of practical and modeling assumptions that constrain the system design. Together, these components establish the basis for the analytical and simulation methods presented in subsequent chapters.

3.2.1 Overview of satellite and UE design

The link analyzed in this study involves a direct connection between a LEO satellite and a handheld UE, forming a critical component of emerging NTN architectures. The design of both the satellite and the user terminal significantly impacts link budget performance, particularly in terms of antenna gain, signal strength, tracking capability, and overall link stability. This section provides a structural overview of both ends of the communication link, emphasizing practical design elements and challenges inherent in LEO-based NTN systems.
This report refers to 3 main satellite-UE systems as indicated by figures 3.2, 3.3 and 3.4.

3.2.1.1 Design Overview

The satellite operates in LEO, typically at an altitude of about 550 km, thereby allowing for lower latency and path loss compared to GEO or MEO satellites. It functions as a regenerative satellite capable of modulation/demodulation, switching/routing and other functions performed at the base station,

Some key considerations of the satellite include:

- Antenna System: The satellite is equipped with a directional high-gain antenna array (usually a phased array) to enable electronic beam steering. This allows real-time tracking of different users and beam-shaping based on the traffic load and the location of the user [2].
- RF front end: The satellite is designed to operate in Ku band (discussed further in section 3.2.2) and consists of amplifiers, low noise amplifier, filters, up-converter and down-converter.
- The satellites are placed at a separation of 20 degrees.

3.2.2 Frequency Band Selection

The frequency band selected for this study plays a vital role in shaping the performance, feasibility and reliability of the satellite communication link. This system architecture focuses on an uplink frequency of 14.5 GHz and a downlink frequency of 10.75 GHz which fall within the centimeter (cm) wave range of Ku band (7-15 GHz) range. These frequencies were selected keeping in mind the acceptable range for modern non-terrestrial network designs while also exploring a relatively unused part of the spectrum for this specific scenario. It offers a balance between the available bandwidth and data rates, antenna design considerations and feasible operating conditions for a handheld UE.

3.2.2.1 Justification

- This band is allocated for Fixed Satellite Service (FSS) and Mobile Satellite Service (MSS), in LEO based systems. They are in line with the current and future spectrum usage trends as addressed in [13].
- The 7-15 GHz range allows for compact and efficient antenna design on both the satellite and UE terminal side. It supports antennas with higher gain and smaller apertures, when compared to L or S band [2].
- This frequency range being in the Ku band, is less susceptible to rain attenuation when compared to Ka band (26-40 GHz). This makes it more convenient for users who are in motion between different environmental conditions.
- These frequencies also allow sufficient bandwidth to support a decent broadband connection with relatively high data rates, without being too affected by path loss or ionospheric losses.

3.2.2.2 Tradeoffs

- While these frequencies do better than Ka band in terms of rain attenuation, it is still a major attenuation factor for frequencies above 10 GHz which must be accounted for. ITU recommendation documents have been used to calculate the attenuation for the purpose of accurate simulation of the link budget.
- At 10.75 GHz and 14.5 GHz. the Doppler shift caused by the rapid motion of the LEO satellite is not negligible and must be compensated for. The simulation includes dynamic Doppler estimation as a function of slant range and the satellite velocity.

The chosen frequencies, 14.5 GHz for UL and 10.75 GHz for DL, represent a sound configuration for satellite communication between a LEO satellite and a handheld UE. This range balances its tradeoffs with better antenna design capabilities and performance characteristics making them a great addition to the existing frequency bands being used for current and next-generation NTN deployments. The calculations and simulations carried out in this study rely heavily on this spectrum selection and forms the basis for this study and its development.

3.3 Software tools and simulation setup

This section details the tools and simulation environment used to implement and analyze the link budget model for LEO satellite communication system. The simulation was carried out using MATLAB because of its ease of use, builtin toolboxes and versatility in visualization. A custom framework was developed to calculate the received power, C/N_0 and other performance parameters along with comparison plots. The input parameters and equations used are based on various reference materials such as textbooks, technical articles and standardization recommendations.

3.3.1 Description of MATLAB for Link Budget Calculation

MATLAB was used as the main tool for calculating the link budget and simulating the various link scenarios due to the following advantages:

- Flexible computing capabilities which help in calculation of link equations and channel parameters.
- Built-in functions for trigonometric operations and various conversions such as from degrees to radians which are essential in the calculations.
- Easy to use visualization tools for plotting curves and analyzing the results better.
- Modular scripting allowing for the reuse of equations at different instances.
- Compatibility with ITU-R recommendation data, which helps to have a comparison metric for calculation of rain attenuation etc.

Custom MATLAB scripts were created to calculate key parameters including:

- Free Space Path Loss

- Atmospheric and rain attenuation
- Received power
- C/N_0 and CNR
- Doppler shift and propagation delay

These parameters were calculated across a range of elevation angles for both the uplink and downlink conditions, enabling a holistic view of the communication link between a LEO satellite and the UE.

3.4 Satellite and User Positioning in Earth-Centered Earth-First(ECEF) Coordinates

To model realistic satellite communication geometry, this thesis uses the ECEF coordinate system to define the positions of both the UE and the satellites. ECEF is a 3D Cartesian coordinate system that rotates with respect to the Earth and is well suited for simulating line-of-sight (LoS), slant range, and Doppler effects in satellite-to-ground communication.

3.4.1 Coordinate System Definition

The ECEF system is defined as follows:

- X-axis: Points from the center of the Earth to the intersection of the Equator and the Prime Meridian (0° latitude, 0° longitude).
- Y-axis: Points from the center of the Earth toward 0° latitude and 90° East longitude.
- Z-axis: Points from the center of the Earth toward the North Pole (90° latitude).

All positions are expressed in meters from the center of the Earth.

3.4.2 Satellite Positioning

In the simulation, a simplified constellation of a LEO satellite is placed around the fixed UE location (Gothenburg, Sweden). This setup is divided into 3 cases as discussed below:

- Case 1 (Figure 3.2): A baseline case with 1 LEO satellite and a single UE with 4 antenna elements.
- Case 2: A comparison scenario -
  - Case 2a: A single satellite with 8 satellite antenna elements and a single UE with 1 UE antenna element
  - Case 2b (Figure 3.3): 4 satellites with 2 antenna elements each and a single UE with 1 UE antenna element.

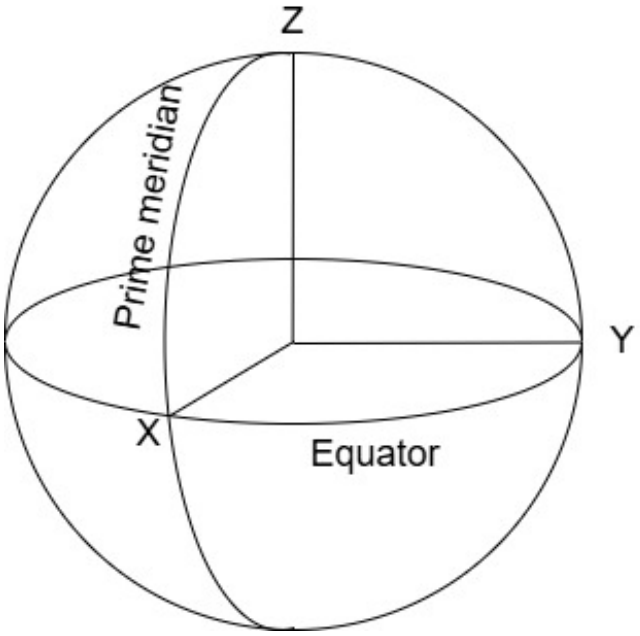

Figure 3.1: Earth Center Earth First co-ordinate system.

It is worth noting that this case does not make any considerations on the UE side, for the sake of simplicity.

- Case 3 (Figure 3.4): 4 satellites with 2 antenna elements each and 1 UE with 2 antenna elements

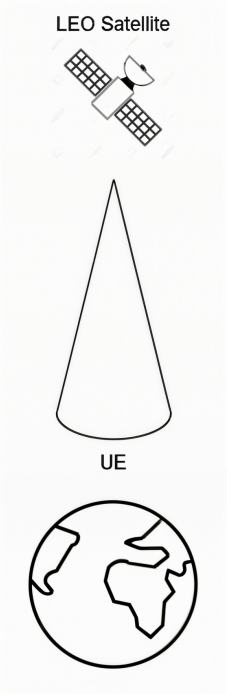

Figure 3.2: System model for Case 1 with 1 LEO stellite and 1 UE.

The satellites are distributed using a small angular offset of 20 degrees in latitude

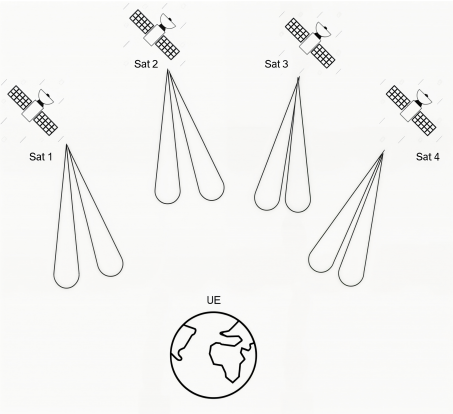

Figure 3.3: System model for case 2b with 4 LEO satellites, each with 2 satellite antenna elements and 1 UE with 1 UE antenna element.

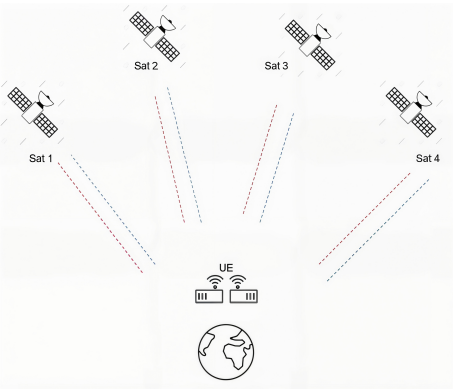

Figure 3.4: System model for Case 3 with 4 LEO satellites, each with 2 satellite antenna elements and 1 UE with 2 UE antenna elements.

from the UE while maintaining the same longitude. While each satellite is placed at a constant altitude (r) above the Earth's surface, the slant range (represented by dotted line in Figure 3.5) of satellite 1 and 4 is around 650 Km. The overall altitude above the Earth's surface can be calculated by

$$r = R_{\mathrm{E}} + H_{\mathrm{sat}}. \tag{3.1}$$

Here, R_{E} is the radius of the Earth and H_{sat} is the altitude of the satellite.

The satellite positions are calculated as

$$x_s = r * cos(\phi_{\mathrm{s}}) * cos(\lambda), \tag{3.2}$$

$$y_s = r * cos(\phi_{\mathrm{s}}) * sin(\lambda), \tag{3.3}$$

and

$$z_s = r * sin(\phi_{\mathrm{s}}). \tag{3.4}$$

Here ϕ_s is the latitude of satellite (degrees) and λ is the longitude of the UE (m).

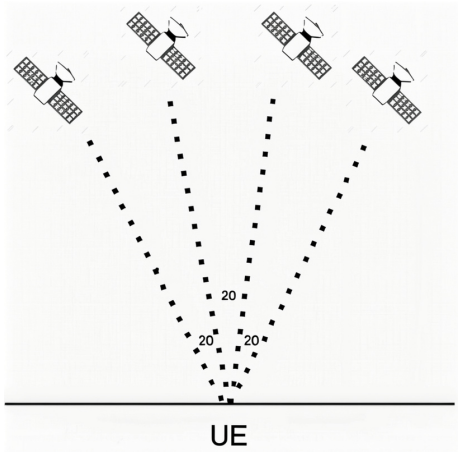

Figure 3.5: Constellation architecture

3.4.3 UE positioning

The UE is assumed to be stationary on the Earth's surface at a fixed latitude and longitude. Its position in ECEF is calculated using equations

$$x_u = R_E * coUE(\phi_{\text{UE}}) * cos(\lambda), \tag{3.5}$$

$$y_u = R_E * cos(\phi_{\text{UE}}) * sin(\lambda) \tag{3.6}$$

and

$$z_u = R_E * sin(\phi_{\text{UE}}) \tag{3.7}$$

where ϕ_{UE} is the latitude of UE (degrees).

This model simplifies the user as a point receiver on the Earth's surface.

3.4.4 Slant range and Elevation angle

Once the satellite and UE positions are defined in ECEF, the slant range is computed as the Euclidean distance (d) in

$$d = \sqrt{(x_{\text{s}} - x_{\text{UE}})^2 + (y_{\text{s}} - y_{\text{UE}})^2 + (z_{\text{s}} - z_{\text{UE}})^2}. \tag{3.8}$$

The elevation angle is also derived from the geometry and is used to determine the visibility and quality of each link. These calculations are central to calculating path loss and Doppler shift in later sections.

3.4.5 Advantages

The ECEF positioning framework is essential for:

- Realistic modeling of path length and FSPL
- Accurate Doppler shift calculation
- Beam visibility and elevation-angle filtering
- Support for multi-satellite and multi-antenna simulations

It gives a geometric foundation for the entire simulation workflow.

3.5 Uplink link budget modeling

This section details the framework used to evaluate uplink link performance in 2 configurations:

- SISO (Single-Input-Single-Output) case i.e 1 x 1
- Multi antenna MIMO case i.e 1x4 and 2x4

The aim is to calculate the parameters such as P_{Rx}, C/N_0 and E_{b}/N_0 for each antenna-UE path.

3.5.1 UE transmit antenna array design

Three antenna configurations are evaluated:

- 1×1: One UE transmit antenna to one satellite — baseline case
- 1×4: One UE antenna communicating with four satellites (distributed Rx diversity)
- 2×4: Two UE transmit antennas to four satellites — full MIMO scenario

Each antenna is modeled as a half-wavelength dipole, and the array gain is computed as described in Section 2.4. The UE's EIRP is fixed for all configurations to maintain fairness in comparison.

3.5.2 Satellite receiver parameters

Each satellite is assumed to be equipped with a high-gain receive antenna (38.5 dBi), consistent with NTN guidelines. The system noise temperature is constant, enabling straightforward computation of C/N_0 and CNR, as defined in Section 2.4.

3.5.3 Geometry and Free space path loss

Using ECEF coordinates (section 3.4), satellite and UE positions are defined in 3D space. Satellites are placed in a horizontal arc relative to the UE, and the slant range is calculated accordingly. The FSPL for each path is then computed using the formula from Section 2.4.2.

3.5.4 Per-Link Signal Parameter Calculation

For each UE antenna–satellite pair, the simulation gives:

- P_{Rx} based on EIRP, FSPL, and satellite receiver gain
- C/N_0, using the G/T figure and Boltzmann constant

To simulate real-world variability (e.g., beam misalignment), a small random variation is applied to the gain in each path.

3.5.5 Doppler-Aware Extension

Each satellite's motion induces a distinct Doppler shift, which is computed per path using satellite velocity projections onto the line-of-sight vectors. This models realistic frequency shifts and contributes to Doppler spread, which affects coherence time and synchronization. Doppler shift computation is detailed in Section 3.8.

3.5.6 Link Budget Aggregation and MIMO Combining

Depending on the configuration:

- 1×1 - Only one link is evaluated
- 1×4 / 2×4 - Power and noise metrics from all paths are combined linearly.

This models coherent combining or a best-case diversity scenario, where the system benefits from all available spatial paths.

3.5.7 Adaptive Modulation and Eb/N0 Update

Following the aggregation, the total Eb/N0 is used to select a suitable modulation scheme (see Section 3.10). The selected spectral efficiency is then used to recompute the final Eb/N0 value, ensuring accurate throughput estimation.

3.5.8 Comparative Case Evaluation

To quantify the benefits of MIMO over SISO, the model simulates and compares:

- Received power (P_{Rx})
- Carrier-to-noise ratio (C/N_0)
- Energy-per-bit to noise ratio (E_{b}/N_0)
- Spectral efficiency and data rate

This is done across all three configurations (1×1, 1×4, 2×4). The results are reported in Chapter 4, including both tabular comparisons and visualizations.

3.6 Downlink link budget modeling

This section describes the methodology used to simulate and analyze the downlink (satellite to UE) communication link in a LEO satellite system. The goal is to compute the received power and link quality at the UE, incorporating satellite transmit parameters, geometric losses, UE antenna characteristics, and system noise. The downlink complements the uplink modeling described in Section 3.4 and follows the same coordinate and propagation framework defined in Section 3.5.

3.6.1 Satellite Transmit Configuration

Each satellite is assumed to transmit using a high-gain directional antenna. The EIRP is defined using the standard formulation introduced in Section 2.4, with an additional power back-off applied to reflect hardware nonlinearities or the multi-beam operation. In simulation, the EIRP per satellite is fixed, and all satellites transmit simultaneously to the UE.

3.6.2 UE Receiver Parameters

The user terminal is configured with an antenna array of 2 to 4 elements. The gain of this array is calculated using the array gain formula discussed in Section 2.4.2, based on the number of elements and the gain of a single dipole element. The system noise temperature is computed from the antenna noise and receiver noise figure, following the approach in Section 2.4.

3.6.3 Per-Path Aggregation and MIMO Combining

In configurations involving multiple satellites and/or UE receive antennas, the system performs aggregation across all available signal paths. This models scenarios where the UE performs:

- Coherent combining (idealized)
- Diversity gain across antenna paths

The aggregated P_{Rx} and C/N_0 are computed using linear-scale summation, and final Eb/N_0 is derived accordingly. This procedure builds on the combining method introduced in Section 2.4, but adapted to the multi-path MIMO context.

3.6.4 Downlink Case Comparisons

The model simulates and compares performance across the different receiver configurations:

- 1×1: Single satellite, single UE antenna
- 4x2 Multi-satellite to multi-antenna UE (D-MIMO)

Metrics such as P_{Rx}, C/N_0, Eb/N_0, and spectral efficiency are compared across these cases.

3.7 Doppler aware path modeling

In this simulation, the Doppler shift is modeled to account for the relative motion between the satellites and the UE in the uplink direction. Since LEO satellites move at very high speeds, they introduce significant Doppler shifts. This section describes how Doppler shift is calculated per path between each satellite and each active UE transmit antenna, based on the simplified geometric and velocity model implemented in the code.

3.7.1 Satellite velocity estimation

Each satellite is assumed to move tangentially in orbit. Instead of a full orbital model, the simulation calculates a velocity direction vector by taking the cross product of the satellite's position with the Y-axis. This gives a perpendicular direction to the position of the satellite, simulating orbital motion.

The resulting unit vector is scaled by a constant satellite speed to obtain the velocity vector of the satellite in 3D space.

3.7.2 Doppler calculation per path

For every satellite and UE antenna pair:

- The line-of-sight (LoS) vector is calculated between the satellite and the UE.
- The satellite's velocity is projected onto this LoS direction to get the relative velocity component.
- The Doppler shift is then calculated using

$$f_{\mathrm{D}} = \frac{v_{\mathrm{rel}}}{\lambda}, \tag{3.9}$$

  where v_{rel} is the relative velocity and λ is the UL/DL wavelength.

This gives a unique Doppler shift value for each path. This Doppler-aware modeling makes the model more realistic and lays the foundation for future extensions such as synchronization and demodulation.

3.8 MIMO modeling at UE and satellite

This section describes how MIMO modeling is incorporated into the simulation to reflect the use of multiple antennas at the UE and the satellite. While a full physical-layer channel model is not simulated, the implemented MIMO structure accounts for the presence of multiple signal paths, diversity gain, and power aggregation across antennas and satellite links.

3.8.1 UE-Side MIMO (Transmit Diversity)

The user terminal is modeled with multiple active transmit antennas (typically 2), each transmitting independently to visible satellites. Each transmit antenna creates a unique link to each satellite, resulting in a UE antenna $\times$ satellite path matrix.

For each path:

- The received power is computed individually
- Doppler shift is applied per path
- A small gain variation is added to reflect practical imbalances

This models UE-side spatial diversity, where signals from different antennas can be combined or selected at the satellite to improve overall link robustness and throughput.

3.8.2 Satellite-Side MIMO (Receive Diversity)

Satellites are assumed to either:

- Receive from multiple UE antennas simultaneously (in a 1-to-many model)
- Collaboratively form a distributed MIMO system, where multiple satellites receive signals from the same UE

In both cases, the satellite or ground network performs coherent combining (ideal case) or power-domain aggregation across available paths. No inter-satellite processing is modeled directly, but the structure supports 1×1, 1×4, and 2×4 configurations.

3.8.3 Path-Level Matrix Representation

The simulation uses matrix-based data structures to represent path-level metrics. This allows the system to apply gain or Doppler offset per link and compute total received power by summing across all paths.

3.8.4 Comparison scenarios

To evaluate the impact of MIMO, 1x1, 1x4 and 2x4 configurations of UE and satellite antennas respectively is used. These results are presented in Chapter 4.

3.9 Link budget calculation approach for UL and DL

This section outlines the systematic approach used to compute the link budget for both the uplink (UE to satellite) and downlink (satellite to UE) paths in the simulation. While the specific parameters differ slightly between the two directions, the overall methodology remains consistent and is rooted in the standard link budget formulation introduced in Chapter 2.

3.9.1 Stepwise method

For each direction of calculation, the link budget is computed following the below high-level steps:

- Definition of system parameters - Frequency, bandwidth, antenna gains.
- Geometry, elevation angle and distance calculation - location and slant range.
- Calculate - FSPL, P_{Rx}, system noise temperature.
- Calculate - C/N_0 and E_{b}/N_0.

4

Results

This chapter presents the outcomes of the simulation-based evaluation of satellite communication links using realistic LEO satellite -architecture, link-budget computation, Doppler aware path modeling, spatial diversity, adaptive modulation, and asymmetrical power allocation. The results demonstrate how system design choices affect key performance indicators such as received power, signal quality, BER and data throughput.

4.1 Case 1: Single satellite Link budget analysis

The baseline satellite communication system was configured using parameters derived from 3GPP TR 38.821 standards for LEO satellite communications. Table 4.1 summarizes the fundamental system parameters used throughout the analysis.

This baseline configuration as seen in Table 4.1 serves as the foundation for all subsequent performance analyses and system comparisons in the upcoming sections.

4.1.1 Uplink Performance

The uplink link budget analysis demonstrates the fundamental challenges and capabilities of LEO satellite communications. Table 4.2 summarizes the uplink link budget parameters for a single satellite–UE communication path using QPSK modulation. All physical link parameters are held constant, including UE transmit power, antenna gains, and distance to the satellite. This configuration forms the baseline case for evaluating performance under fixed link conditions.

This configuration yields a C/N_0 of approximately 79.71 dBHz, with a resulting E_b/N_0 of –0.29 dB for QPSK. The corresponding bit error rate under AWGN conditions is estimated at 0.09. This forms the benchmark for assessing how higher-order modulation schemes affect signal robustness under the same physical link conditions.

4.1.2 Impact of Modulation Order on (E_b/N_0) and BER

Table 4.3 presents the impact of increasing modulation order on E_b/N_0 and BER, under fixed transmission conditions. While the physical link remains identical to the QPSK case described above, the spectral efficiency is increased by using 16-QAM and 64-QAM, resulting in higher throughput at the cost of reduced noise tolerance.

Table 4.1: Parameters for Uplink Link Budget Calculation

Parameter	Value	Definition
R_{E}	6378×10^3 m	Radius of Earth
d	6928×10^3 m	Distance to satellite (from Earth's center)
h_{sat}	550×10^3 m	Satellite altitude
c	3×10^8 m/s	Speed of light
f_{up}	14.5×10^9 Hz	Uplink frequency
λ_{up}	0.0207 m	Uplink wavelength
B	50 MHz	System bandwidth
Satellite Parameters		
L_1	11.8°	Satellite longitude
A_{sat}	0.5 (unitless)	Antenna aperture (assumed)
$G_{\mathrm{sat,rx}}$	38.5 dBi	Satellite receive gain
$L_{\mathrm{feeder,rx}}$	3 dB	Feeder loss
T_{A}	150 K	Antenna noise temperature
$T_{\mathrm{e,RX}}$	250 K	Receiver noise temperature
T_{sys}	300 K	System noise temperature
k	-228.6 dBW/Hz/K	Boltzmann constant
UE Parameters		
l_{UE}	57.8°	Location: Säve Airport
L_{ftx}	2 dB	Transmit feeder loss
P_{tx}	3 dBW (33 dBm)	UE transmit power
$EIRP_{\mathrm{UE}}$	13 dBW	Max UE EIRP
$N_{\mathrm{UE,ant}}$	4	UE antenna elements
$g_{\mathrm{UE},1}$	3 dB	Gain per UE antenna
A_{UE}	3.21×10^{-4} m^2	UE antenna area

As shown, increasing the modulation order improves spectral efficiency and data rate. However, this comes with a clear trade-off: the required E_{b}/N_0 increases substantially, and the system becomes more susceptible to noise. For instance, 64-QAM achieves a data rate of 300 Mbps, but suffers a BER of 0.22 under the same link conditions where QPSK achieves 0.09.

These results highlight the importance of adaptive modulation in satellite systems. By adjusting modulation schemes based on real-time link quality, it is possible to optimize performance while maintaining reliability. The thresholds implemented in the simulation (see Chapter 3) are consistent with the trade-offs demonstrated in this table.

4.1.3 Uplink Link Budget Analysis

Figure 4.1 illustrates the variation of Doppler shift and propagation delay with the elevation angle of the satellite in the uplink. As elevation increases from 30° to 90°, the Doppler shift decreases almost linearly from approximately 370 kHz to nearly 0 Hz. This behavior is expected, as the Doppler effect is strongest when the satellite moves tangentially to the UE (at low elevation angles) and weakest when

Table 4.2: Uplink Link Budget Metrics with QPSK Modulation

Parameter	**Value**	**Definition**
Modulation Scheme	QPSK	Digital modulation used
M	4	Modulation order
Spectral Efficiency	2.00 bits/s/Hz	Bits per second per Hz
B	50 MHz	Transmission bandwidth
$G_{\text{sat,rx}}$	38.500 dB	Satellite receive antenna gain
$P_{\text{tx,UE}}$	3.000 dBW	UE transmit power
$G_{\text{UE,tx}}$	9.021 dB	UE transmit antenna gain
$EIRP_{\text{UE}}$	13.000 dBW	UE effective isotropic radiated power
d_{LEO}	562.64 km	Distance to satellite
Slant Range	550.00 km	Range based on elevation angle
Doppler Shift	377,000 Hz	Uplink Doppler frequency offset
Propagation Delay	1.83 ms	One-way propagation delay
L_{FSPL}	170.476 dB	Free space path loss
Rain Loss	4.688 dB	Attenuation due to rain
Additional Losses	5.138 dB	Total extra attenuation
$P_{\text{rx,sat}}$	–124.114 dBW	Received power at satellite
G/T_{sat}	13.729 dB/K	Satellite figure of merit
C/N_0	79.715 dBHz	Carrier-to-noise density ratio
C/N	2.725 dB	Carrier-to-noise ratio
Bitrate	100.000 Mbps	Achievable data rate
E_b/N_0	–0.286 dB	Energy per bit to noise density ratio
BER	0.090	Bit error rate (uncoded system)
SNR	2.72 dB	Signal-to-noise ratio

it is directly overhead.

Figure 4.1 also shows the variation in propagation delay over the same range of elevation angles. As the satellite moves closer to zenith, the slant range decreases, leading to a shorter signal path and lower propagation delay. The delay drops from about 3.4 ms at 30° to approximately 1.8 ms at 90°. These results highlight the importance of considering elevation-dependent timing and frequency offset variations in the design of synchronization and tracking systems for LEO communication links.

Figure 4.2 presents four key link behavior plots as a function of elevation angle, offering a broader view of elevation-related link dynamics in an LEO uplink scenario.

- Time vs. Elevation Angle (Figure 4.2 (a)): The elevation angle of the satellite follows a symmetrical trajectory over time, corresponding to a full pass from rise to zenith and back toward the horizon. This reflects a typical satellite pass duration of approximately 120 seconds.
- Elevation Angle vs. Distance (Figure 4.2 (b)): As the elevation increases, the slant range between the UE and satellite decreases sharply. The distance drops from nearly 1000 km at 30° to approximately 550 km at 90°, significantly impacting free space path loss and link budget.
- Elevation Angle vs. C/N_0 (Figure 4.2 (c)): C/N_0 improves steadily with

Table 4.3: Impact of Modulation Order on Link Performance

Parameter	**QPSK**	**16-QAM**	**64-QAM**
M	4	16	64
Spectral Efficiency	2.00 bits/s/Hz	4.00 bits/s/Hz	6.00 bits/s/Hz
Bitrate	100 Mbps	200 Mbps	300 Mbps
E_b/N_0	–0.286 dB	–3.296 dB	–5.057 dB
BER	0.090	0.150	0.220
Definitions			
M	Modulation order (number of constellation points)		
Spectral Efficiency	Bits transmitted per second per Hz of bandwidth		
Bitrate	Achievable data rate for fixed bandwidth		
E_b/N_0	Energy per bit to noise power spectral density ratio		
BER	Bit error rate at given E_b/N_0		

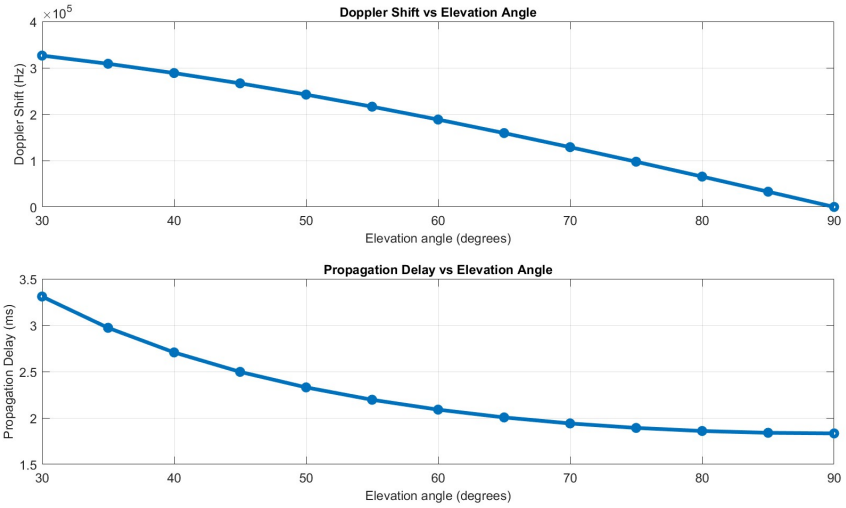

Figure 4.1: Effect of elevation angle on Doppler shift and propagation delay (Uplink)

increasing elevation angle. This is primarily due to reduced path loss at shorter distances, resulting in higher received power. C/N_0 increases from around 74 dBHz to nearly 80 dBHz.

- Elevation Angle vs. Bit Error Rate ((Figure 4.2 (d)): The bit error rate (BER) decreases substantially with elevation angle. At low elevations, higher path loss and Doppler shift result in degraded E_b/N_0 and thus higher BER. As elevation approaches 90°, the BER falls below 0.05, confirming improved signal robustness.

These plots collectively demonstrate the importance of satellite elevation angle in determining uplink communication performance. They validate the dynamic behavior of signal quality over a satellite pass and justify the inclusion of elevation-aware metrics in adaptive modulation and scheduling decisions.

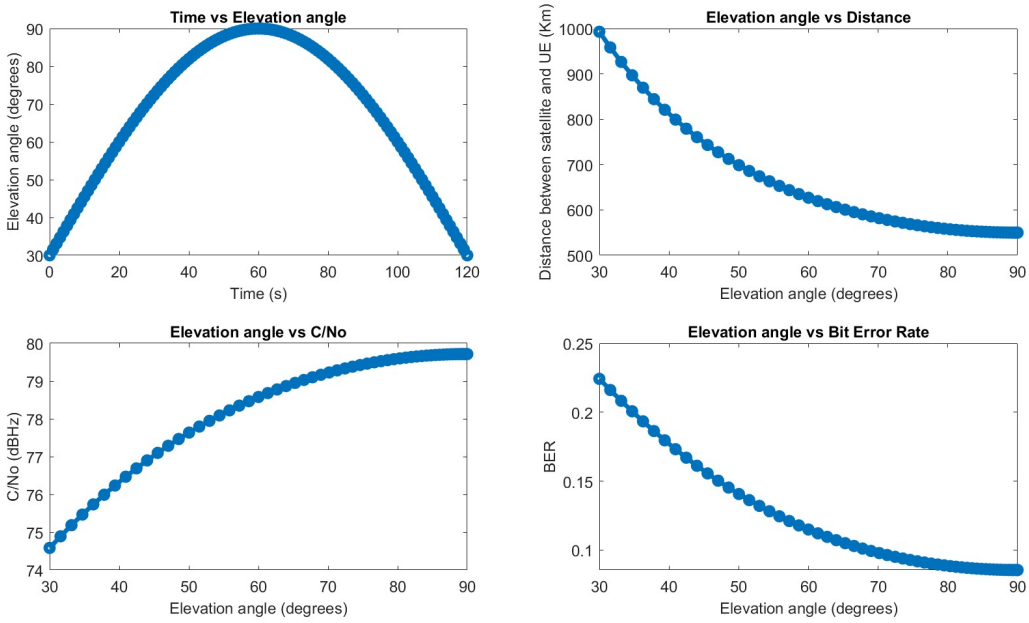

Figure 4.2: Impact of elevation angle on link dynamics (Uplink): Elevation vs. time, distance, C/No, and BER

4.1.4 Downlink Performance

The baseline parameters assumed in the downlink link budget of Case 1 is depicted in Table 4.4.

Table 4.5 presents the detailed link budget parameters for the downlink scenario using QPSK modulation. All satellite, channel, and user-side parameters are held constant, and only the modulation scheme is varied in further analysis. These values represent the baseline configuration for understanding the downlink behavior under LEO conditions.

This QPSK configuration reflects a relatively low spectral efficiency but demonstrates the robustness of lower-order modulation under weak link conditions. The resulting E_b/N_0 of –9.15 dB yields a BER of approximately 0.31, which is significantly higher than what is typically acceptable in practice. However, it establishes a baseline for comparing more efficient, albeit more error-prone, modulation schemes.

4.1.5 Downlink Link Budget Analysis

Figure 4.3 illustrates the variation in Doppler shift and propagation delay with respect to satellite elevation angle in the downlink. The Doppler shift decreases approximately linearly from 250 kHz at 30° to near-zero at 90°, due to reduced projection of satellite velocity onto the line-of-sight vector.

The propagation delay also reduces from about 3.4 ms to 1.8 ms as elevation increases, reflecting a shortening slant range. This behavior directly affects frame alignment and synchronization accuracy in time-sensitive LEO applications.

Table 4.4: Parameters for Downlink Link Budget Calculation

Parameter	Value	Definition
R_{E}	6378×10^3 m	Radius of Earth
d	6928×10^3 m	Distance to satellite (from Earth's center)
h_{sat}	550×10^3 m	Satellite altitude
c	3×10^8 m/s	Speed of light
f_{down}	10.75×10^9 Hz	Downlink frequency
λ_{down}	0.0279 m	Wavelength at f_{down}
B	50 MHz	System bandwidth
UE Parameters		
UE Latitude (l)	57.8°	Säve Airport
N_{ue}	4	UE antenna elements
$g_{\mathrm{ue},1}$	3 dB	Gain per UE antenna
$G_{\mathrm{UE,rx}}$	9.02 dB	Total UE receive gain
A_{ue}	4.32×10^{-4} m^2	Estimated UE antenna area
System Noise Parameters		
T_A	150 K	Antenna noise temperature
NF	1.2 dB	Noise figure
F	1.32 (linear)	Noise factor
T_{rx}	92.8 K	Receiver noise temperature
T_{sys}	242.8 K	Total system noise temperature
T_0	290 K	Reference temperature
k	−228.6 dBW/Hz/K	Boltzmann constant (log scale)
Satellite Parameters		
η	0.6	Antenna efficiency
L_1	11.8°	Satellite longitude
$EIRP_{\mathrm{dens}}$	4 dBW/MHz	EIRP density

Figure 4.4 provides further analysis of downlink link behavior with changing elevation. The subplots show:

- Time vs Elevation (Figure 4.4 (a)): Satellite elevation follows a symmetric arc across the pass duration.
- Elevation vs Distance (Figure 4.4 (b)): Slant range decreases from nearly 1000 km to 550 km as elevation increases.
- C/N_0 (Figure 4.4 (c)): Carrier-to-noise density improves from 66 to nearly 71 dBHz due to reduced path loss.
- BER (Figure 4.4 (d)): Bit error rate reduces steadily from 0.39 to 0.30, aligning with higher E_{b}/N_0 at better elevation.

These plots emphasize the need for elevation-aware adaptation in modulation and scheduling. As signal quality improves at higher elevation angles, more efficient modulation can be used, while lower elevations may require fallback to robust schemes like QPSK.

Table 4.5: Downlink Link Budget Metrics with QPSK Modulation

Parameter	Value (QPSK)	Definition
Modulation Scheme	QPSK	Digital modulation type
M	4	Modulation order (constellation size)
Spectral Efficiency	2.00 bits/s/Hz	Bits per second per Hz of bandwidth
B	50.00 MHz	Transmission bandwidth
$G_{\text{UE,rx}}$	9.021 dB	UE receive antenna gain
EIRP_{sat}	20.990 dBW	Satellite effective isotropic radiated power
G_{sat}	38.500 dBi	Satellite antenna gain
Slant Range	562.64 km	Distance from UE to satellite
Elevation-Based Distance	550.00 km	Range based on elevation geometry
Doppler Shift	279,500 Hz	Downlink Doppler frequency offset
Propagation Delay	1.83 ms	Signal delay from satellite to UE
L_{FSPL}	167.877 dB	Free space path loss
Additional Losses	–3.960 dB	Other link gains (e.g., negative loss for favorable conditions)
$P_{\text{rx,UE}}$	–133.907 dBW	Power received at UE antenna
G/T_{UE}	–14.823 dB/K	UE figure of merit
C/N_0	70.850 dBHz	Carrier-to-noise power spectral density
C/N	–6.140 dB	Carrier-to-noise ratio
Bitrate	100.000 Mbps	Achievable throughput
E_b/N_0	–9.150 dB	Energy per bit to noise density ratio
BER	0.31	Bit error rate
SNR	–6.14 dB	Signal-to-noise ratio

4.1.6 Impact of Satellite Antenna Count on Received Power

Figure 4.5 illustrates the variation in received power at the UE as a function of the number of antenna elements employed in the UE array, under different per-element gain assumptions: 1 dB, 3 dB, and 5 dB.

As anticipated, the received power increases logarithmically with the number of UE antenna elements, attributed to the cumulative array gain. Each curve represents a fixed per-element gain and exhibits a clear upward trend, with higher starting power levels observed for larger individual element gains. It also reinforces the advantages of implementing beamforming or D-MIMO techniques at the satellite. However, the gains begin to saturate beyond 24 elements, suggesting diminishing returns. The result supports using a moderate number of transmit elements for a practical trade-off between performance and hardware complexity.

4.2 Case 2: Comparing Large vs Distributed Satellites with Multiple Antennas

This section presents a comparative analysis between two deployment scenarios:

- **Case 2a**: A single large satellite with 8 satellite antenna elements and single UE antenna
- **Case 2b**: Four smaller satellites, each equipped with 2 satellite antenna elements and single UE antenna

The analysis is conducted for both uplink and downlink, with metrics evaluated over a sweep of elevation angles from 30° to 90°. The goal is to assess how distributed

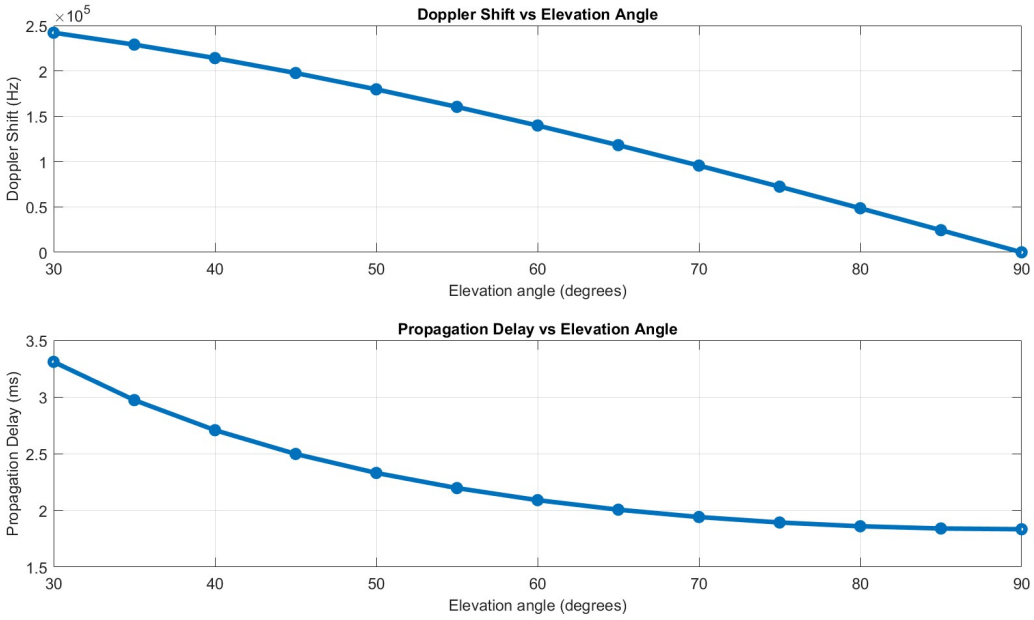

Figure 4.3: Effect of elevation angle on Doppler shift and propagation delay (Downlink)

architectures perform in terms of received power, signal quality, and propagation behavior compared to monolithic designs.

4.2.1 Uplink Performance Analysis

Figure 4.6 shows a detailed comparison between Case 2a and Case 2b for uplink metrics:

- Received Power (Figure 4.6 (a)): Case 2b (4 small satellites) achieves slightly lower received power due to EIRP back-off, but compensates through ideal combining of multiple independent paths.
- C/N_0 and E_b/N_0 (Figure 4.6 (b) and (c)): C/N_0 is higher for Case 2a due to concentrated transmit power and higher G/T. However, in Case 2b, the diversity gain improves overall E_b/N_0 slightly, particularly at higher elevations.
- FSPL and Slant Range (Figure 4.6 (d) and (e)): These remain identical across both cases, as the geometric link to the UE is the same.

4.2.2 Downlink Performance Analysis

Figure 4.7 illustrates the downlink comparison. The results follow similar trends as in the uplink:

- Power and C/N_0 (Figure 4.7 (a) and (b)): The large satellite consistently delivers higher P_{rx} and C/N_0 due to larger antenna gain and higher power per stream.

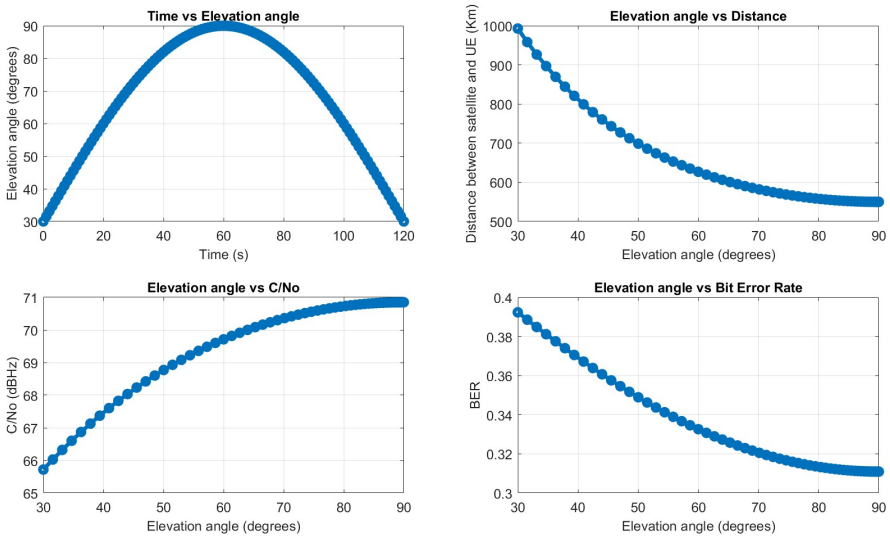

Figure 4.4: Impact of elevation angle on link dynamics (DL)

- Eb/N0 (Figure 4.7 (c)): At higher elevations, Case 2b approaches Case 2a performance due to reduced FSPL and improved diversity.

4.2.3 Effect of Antenna Count and Satellite Count

Figures 4.8 and 4.9 show how increasing the number of antennas per satellite influences C/N_0 for various satellite counts. While C/N0 improves with more antennas, the gains show diminishing returns after 12 antennas. The improvement is steeper with more satellites due to power diversity and spatial separation, but hardware and power constraints limit the practicality of very large arrays.

4.2.4 Doppler Shift and Delay Comparison

Figure 4.10 shows the Doppler shift and propagation delay for both uplink and downlink. As expected, Doppler shift (Figure 4.10 (a)) decreases with elevation, and uplink experiences higher Doppler (∼370 kHz) compared to downlink (∼280 kHz). Propagation delay (Figure 4.10 (b)) also decreases from ∼3.4 ms to ∼1.8 ms as the elevation approaches zenith.

These dynamics highlight the need for Doppler tracking and delay compensation, especially in real-time services with bursts.

4.3 Case 3: D-MIMO Simulation with 4 Satellites and 2 UE Antennas

This simulation models a D-MIMO scenario as seen in Figure 3.4. This setup involves the use of 4 satellites with a 20° separation and 2 antenna elements each. The UE in this setup has 2 antenna elements which gives a total of 8 paths or communication

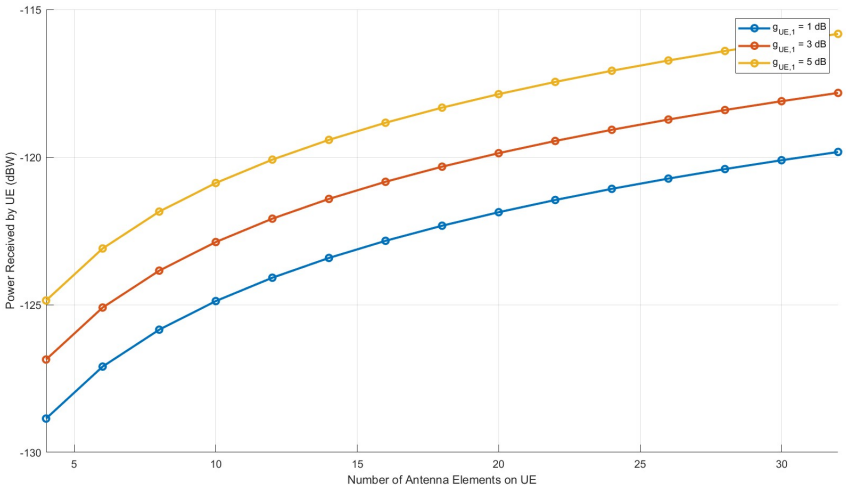

Figure 4.5: Power received by UE vs. number of satellite antenna elements (Downlink)

links between the satellite and the UE. Each path transmits independent data, and link parameters such as Doppler shift, power, BER, and spectral efficiency are calculated on a per-stream basis.

4.3.1 Uplink Performance Analysis

4.3.1.1 Simulation Parameters

This section outlines the physical and system-level assumptions used in the Case 3a uplink simulation. The simulation parameters are described in Table 4.6.

4.3.1.2 Doppler Shift Per Path

Doppler shift was calculated individually for each satellite–antenna stream by projecting the satellite's velocity onto the line-of-sight vector to the UE. It reflects the time-varying frequency offset introduced by satellite motion in LEO. The Doppler shift observed for each path of the communication link is indicated in Table 4.7.

4.3.1.3 Received Power and BER per Path

Table 4.8 summarizes the signal power received at the satellite for each UE antenna stream and its corresponding BER. Power levels vary due to path loss and antenna asymmetry, influencing per-stream reliability.

4.3.1.4 UL Link Budget Metrics

This section compiles key link budget components elevation angle, FSPL, C/N_0, and E_b/N_0 to quantify link quality for each uplink path. The final link budget metrics for case 3a are shown in Table 4.9.

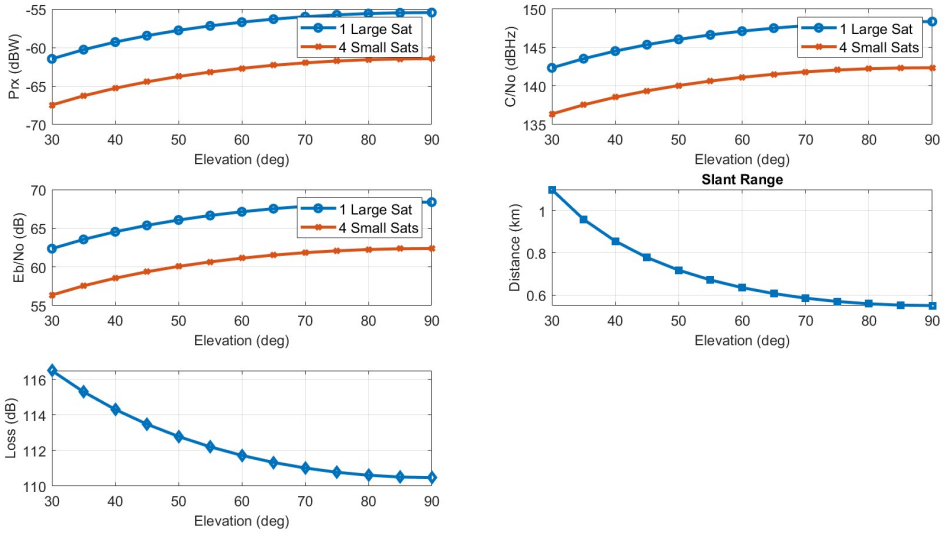

Figure 4.6: Uplink comparison for Case 2(a) and Can 2(b)

4.3.1.5 Throughput Summary

Using adaptive modulation based on E_b/N_0 thresholds, each stream is assigned a spectral efficiency using a threshold rule mentioned in Section 2.4.9.2. The total data rate is computed by summing all stream-wise rates, offering a practical estimate of D-MIMO uplink throughput.

Based on this rule and the E_b/N_0 :

- Total Uplink D-MIMO Data Rate: 400 Mbps
- Average Spectral Efficiency: 2.0 bps/Hz

This result demonstrates the capability of D-MIMO architectures in achieving high throughput even under variable geometry, asymmetric power, and Doppler shifts, although per-stream reliability is strongly influenced by satellite position and antenna power allocation.

4.3.2 Downlink Performance Analysis

Here, a D-MIMO downlink scenario is modeled where four satellites transmit independently to a user terminal with two receive antennas. Power asymmetry is introduced across satellites, and performance is evaluated per stream based on Doppler shift, link budget, BER, and adaptive modulation.

4.3.2.1 Simulation Parameters

This section outlines the system setup for downlink D-MIMO evaluation. It includes satellite-side EIRP configurations, UE antenna characteristics, channel bandwidth, and the adaptive modulation logic used to determine throughput.

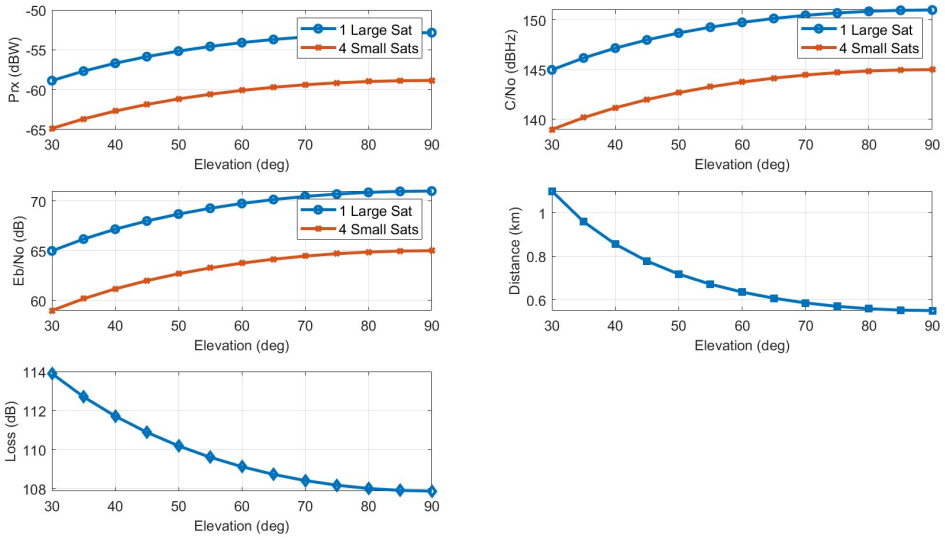

Figure 4.7: Downlink comparison for Case 2a and Case 2b

4.3.2.2 Doppler Shift per Path

Doppler shifts were calculated for each satellite–UE antenna combination based on satellite velocity and geometry. These shifts introduce frequency offsets that must be tracked in practical downlink receivers for accurate demodulation.

4.3.2.3 Asymmetrical Power Allocation

In our study, asymmetric power allocation is implemented to reflect realistic scenarios in satellite communication networks, where satellites may transmit at varying power levels due to design constraints, power sharing, or adaptive optimization strategies. Instead of assuming uniform transmit power across all satellites, a fixed offset in EIRP is applied to each satellite using a predefined vector of weights. This simulates a non-uniform downlink as depicted in Table 4.12, where certain satellites transmit with either power boosts or reductions relative to a baseline. Such an approach allows for analysis of its impact on UE reception quality, signal-to-noise ratios, and ultimately data throughput. It also enables exploration of how system-level performance responds to practical variations in satellite transmit behavior, supporting more robust and flexible D-MIMO system design.

4.3.2.4 Received Power and BER per path

This table presents P_{rx} and BER for each satellite-to-UE stream. Power varies due to asymmetrical EIRP and path loss, while BER depends on the effective SNR at each receiver input.

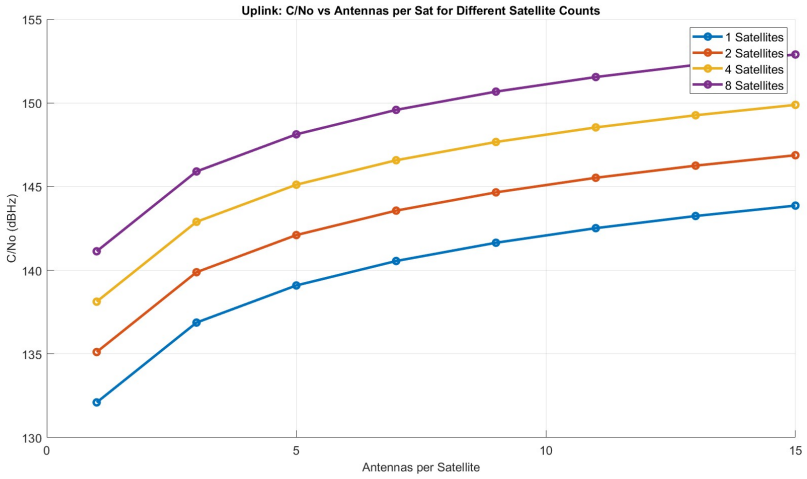

Figure 4.8: C/No vs. number of antennas per satellite for varying satellite counts (uplink)

4.3.2.5 DL Link budget Metrics

This section compiles FSPL, elevation angle, C/N_0, and E_b/N_0 per link, offering a detailed view of signal quality for each stream. These values are essential for determining the achievable data rates using adaptive modulation.

4.3.2.6 Throughput Summary

Based on the calculated E_b/N_0, each stream is assigned a spectral efficiency level based on adaptive modulation thresholds mentioned in Section 2.4.9.2.

The combined data rate across all downlink streams reflects the effectiveness of the D-MIMO system in leveraging spatial diversity and link adaptation.

Only two stream exceeds 6 dB E_b/N_0 (Sat 4, Ant 1 and Sat 4, Ant 2), while others operate at lower spectral efficiencies.

The observed saturation in downlink throughput is primarily due to bottlenecks introduced by UE constraints such as limited receive antennas, processing capability. As the satellite increases its antenna count, the UE is unable to fully exploit the added spatial resources, resulting in diminishing returns despite the growing transmit diversity.

4.3.2.7 Impact of Antenna Scaling

This section evaluates how increasing the number of antenna elements on each satellite affects the overall downlink performance. By recalculating the link budget for varying antenna counts (from 1 to 64), the system's E_b/N_0 and corresponding spectral efficiency are estimated. The results as seen in Table 4.15 demonstrate clear performance gains up to 8–16 antennas, after which improvements taper off—highlighting diminishing returns beyond a certain hardware threshold.

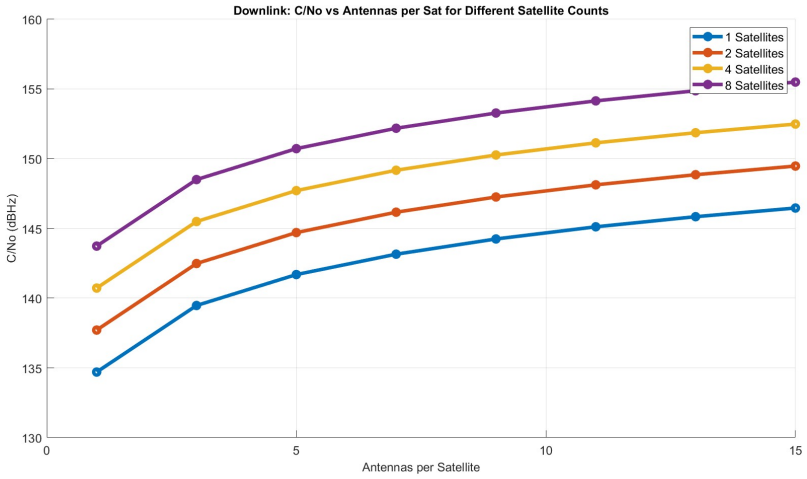

Figure 4.9: C/No vs. number of antennas per satellite for varying satellite counts (downlink)

As seen in Figure 4.11, spectral efficiency increases rapidly up to 8 antennas and saturates beyond 16, highlighting diminishing returns in practical D-MIMO configurations. The observed saturation in downlink throughput beyond 16 antennas is primarily due to bottlenecks introduced by UE constraints such as limited receive antennas, processing capability. As the satellite increases its antenna count, the UE is unable to fully exploit the added spatial resources, resulting in diminishing returns despite the growing transmit diversity.

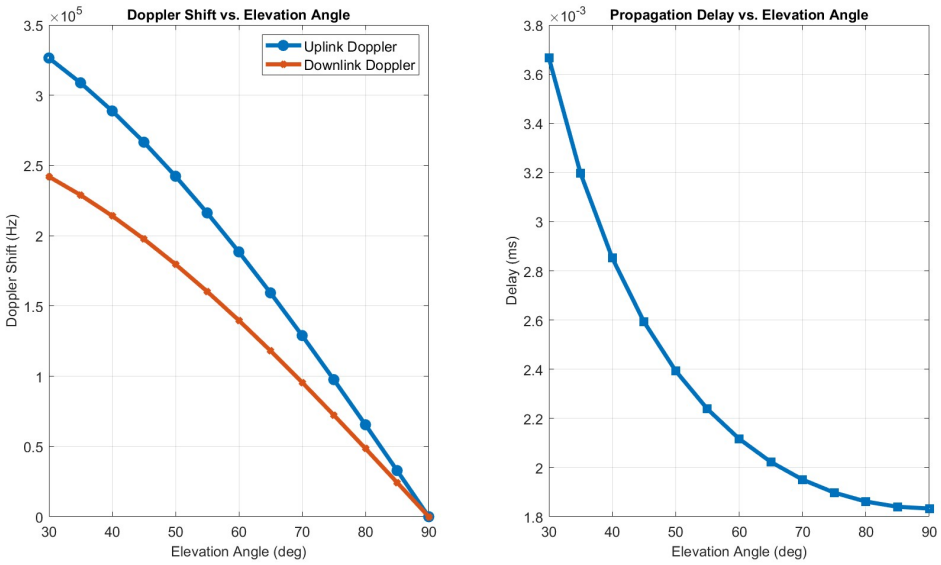

Figure 4.10: Doppler shift and propagation delay vs. elevation angle (uplink and downlink)

Table 4.6: Simulation Parameters for Case 3a: Uplink D-MIMO

Parameter	**Value**	**Definition**
Number of Satellites	4	Satellites are distributed around the UE for D-MIMO uplink
UE Antennas	2	Active transmit antennas with asymmetric power allocation
Carrier Frequency	14.5 GHz	Uplink operating frequency
Bandwidth	50 MHz	Communication bandwidth used for transmission
Modulation Scheme	Adaptive (QPSK, 16-QAM)	Scheme selected per path based on Eb/N0
UE Antenna Gain	9.02 dBi	Gain of each UE transmit antenna element
Satellite Rx Gain	38.5 dBi	Receiving antenna gain of each satellite
Noise Temperature	300 K	Assumed system noise temperature
Power Allocation	0 dB, –3 dB	Relative EIRP offset for UE antennas 1 and 2
UE Transmit Power	3 dBW	Total transmit power; corresponding EIRP is 13 dBW
UE Power Weights	[0 –3]	Power offset vector applied to two antennas

Table 4.7: Doppler Shift per Satellite and UE Antenna (Hz)

Satellite	UE Antenna	Doppler Shift (Hz)
1	1	+368227.50
1	2	+368227.50
2	1	+371409.76
2	2	+371409.76
3	1	-369747.88
3	2	-369747.88
4	1	-363644.52
4	2	-363644.52

Table 4.8: Received Power and Bit Error Rate per Stream

Satellite	UE Antenna	P_{rx} (dBW)	BER
1	1	-131.53	0.1740
1	2	-134.64	0.2910
2	1	-121.38	0.0660
2	2	-125.95	0.0340
3	1	-123.42	0.0310
3	2	-125.51	0.1230
4	1	-131.36	0.2600
4	2	-134.62	0.3490

Table 4.9: Per-Stream Link Budget Values

Sat.	Ant.	Elevation (deg)	FSPL (dB)	P_{rx} (dBW)	C/N0 (dBHz)	Eb/N0 (dB)
1	1	13.21	183.30	-131.53	75.61	-4.39
1	2	13.21	183.30	-134.64	71.80	-8.20
2	1	43.05	173.79	-121.38	80.19	0.19
2	2	43.05	173.79	-125.95	81.57	1.57
3	1	43.05	173.79	-123.42	82.26	2.26
3	2	43.05	173.79	-125.51	78.47	-1.53
4	1	13.21	183.30	-131.36	72.75	-7.25
4	2	13.21	183.30	-134.62	68.83	-11.17

Table 4.10: Simulation Parameters for Case 3b: Downlink D-MIMO

Parameter	Value	Definition
N_{sat}	4	Number of LEO satellites
$N_{\text{UE,rx}}$	2	Number of UE receive antennas
f_{carrier}	10.75 GHz	Downlink carrier frequency
B	50 MHz	Transmission bandwidth
Noise Figure / T_{sys}	1.2 dB / 300 K	UE noise figure and system temperature
Modulation Scheme	Adaptive (QPSK, 16-QAM)	Dynamic based on link conditions
EIRP_{sat} (baseline)	37 dBW	Satellite EIRP per beam (before weighting)
Power Weights	[0, 1, –2, 3] dB	Asymmetric satellite power allocation
$G_{\text{UE,rx}}$	9.02 dBi	UE receive antenna gain

Table 4.11: Downlink Doppler Shift per Satellite and UE Antenna

Satellite	UE Antenna	Doppler (Hz)
1	1–2	–254,804.49
2	1–2	–215,271.21
3	1–2	+214,307.98
4	1–2	+251,633.18

Table 4.12: Asymmetrical Power Allocation per Satellite

Satellite	Power Offset (dB)	Effective EIRP (dBW)
1	+0	37.00
2	+1	38.00
3	-2	35.00
4	+3	40.00

Table 4.13: Received Power and Bit Error Rate per Stream

Satellite	UE Antenna	P_{rx}(dBW)	BER
1	1	-134.75	0.3630
1	2	-135.02	0.2870
2	1	-125.91	0.0690
2	2	-125.47	0.1330
3	1	-128.85	0.1800
3	2	-128.43	0.2090
4	1	-131.69	0.2750
4	2	-131.77	0.2710

Table 4.14: DL Link Budget Metrics

Sat.	Ant.	Elevation (deg)	FSPL (dB)	P_{rx} (dBW)	C/No (dBHz)	Eb/N0 (dB)
1	1	13.40	180.58	-134.75	69.79	-10.21
1	2	13.40	180.58	-135.02	72.06	-7.94
2	1	35.43	172.61	-125.91	80.57	0.57
2	2	35.43	172.61	-125.47	78.08	-1.92
3	1	35.43	172.61	-128.85	76.77	-3.23
3	2	35.43	172.61	-128.43	75.69	-4.31
4	1	13.40	180.58	-131.69	72.82	-7.18
4	2	13.40	180.58	-131.77	72.45	-7.55

Table 4.15: Effect of Increasing Satellite Antennas on E_{b}/N_0 and Data Rate

Number of Antennas	E_{b}/N_0 (dB)	Spectral Efficiency (bps/Hz)
1	-2.18	1.00
2	0.83	1.00
4	3.84	2.00
8	6.85	4.00
16	9.86	4.00
32	12.87	4.00
64	15.88	4.00

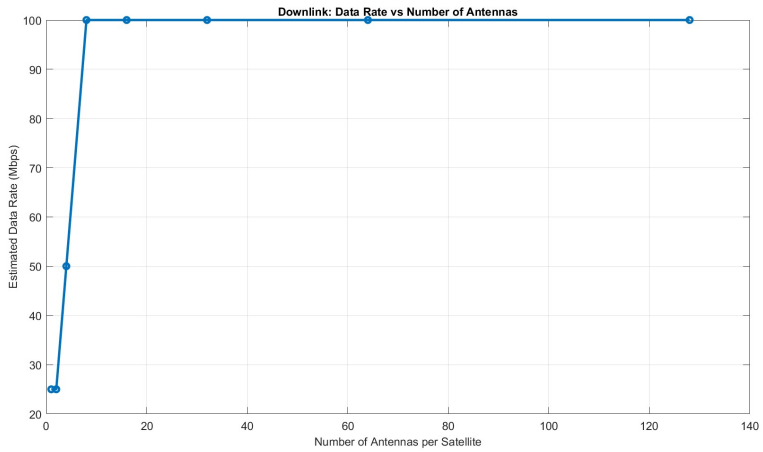

Figure 4.11: Downlink Throughput vs. Number of Antennas per Satellite

5

Conclusion

This thesis focused on building a comprehensive and scalable framework for cm-wave link budget modeling in satellite communication systems, with a gradual transition from conventional single-satellite setups to more advanced D-MIMO architectures. Rather than proving the feasibility of D-MIMO outright, the aim was to explore how fundamental link parameters behave under practical constraints and how system complexity scales when moving toward futuristic multi-antenna, multi-satellite designs.

Beginning with single-satellite uplink and downlink link budget calculations, the study expanded to include detailed modeling of Doppler effects, elevation-based dynamics, asymmetrical power allocation, and adaptive modulation. Bit-level simulations and spectral efficiency mapping provided deeper insights into the limitations and trade-offs of cm-wave satellite links, particularly under LEO conditions.

Through progressive refinement of the simulation architecture, this work demonstrates how such a framework could be instrumental in evaluating and guiding future 6G research, especially for NTN that are expected to operate at high frequencies, support mobility, and require spatial diversity for throughput and coverage.

Ultimately, this thesis contributes a modular and adaptable platform for analyzing cm-wave satellite links, which can serve as a foundation for evaluating advanced NTN proposals and system-level planning in upcoming 6G standardization and deployments.

6

Future Work

While this thesis demonstrates the feasibility and advantages of D-MIMO in LEO satellite communications, several research directions remain open for further exploration and enhancement:

- Full-Fledged Physical (PHY)/Media Access Control (MAC) Layer Integration: The current implementation focuses primarily on link budget, modulation, and bit-level simulation. Extending the model to include PHY layer impairments like phase noise, synchronization overhead, and MAC-level scheduling would allow end-to-end system-level validation.
- Channel Models with Fading and Shadowing: Future work could incorporate more realistic channel models, including Rician or Nakagami fading and terrain-based shadowing, to assess performance under real-world propagation conditions.
- Uplink Power Control and Beamforming: Implementing smart power control schemes at the UE, as well as dynamic beam steering at the satellites, could enhance the spectral efficiency and fairness across the network.
- Network-Wide Coordination: This thesis models D-MIMO per UE. Future efforts could expand to multi-user and multi-cell environments with coordinated satellite constellations, optimizing inter-satellite links (ISLs) and resource sharing.
- Mobility and Handover Management: Satellite passes and fast-changing geometry require seamless handover schemes. Future work could study how D-MIMO systems handle rapid UE mobility and Doppler variations across overlapping coverage areas.
- Machine Learning for Adaptation: Adaptive modulation, power allocation, and antenna selection could be further optimized using data-driven approaches, especially under uncertain or highly dynamic channel conditions.
- Downlink Precoding and Channel State Information (CSI) Feedback: For D-MIMO in the downlink, future research could implement and evaluate linear/nonlinear precoding techniques under imperfect CSI feedback scenarios.
- Hardware Validation and Emulation: To transition from simulation to deployment, prototyping using Software Defined Radio (SDR) platforms or satellite emulators could help validate D-MIMO designs in real-time environments.

Bibliography

[1] Ericsson, *Ericsson Mobility Report: Mobile data traffic increased almost 300-fold over 10 years*, November 2021. [Online]. Available: https://www.ericsson.com/en/press-releases/2021/11/ericsson-mobility-report-mobile-data-traffic-increased-almost-300-fold-over-10-years.

[2] S. Chen, Y.-C. Liang, S. Sun, S. Kang, W. Cheng, and M. Peng, "Vision, Requirements, and Technology Trend of 6G: How to Tackle the Challenges of System Coverage, Capacity, User Data-Rate and Movement Speed," *IEEE Wireless Communications*, vol. 27, no. 2, pp. 218–228, 2020.

[3] 3GPP, *Study on channel model for frequencies from 0.5 to 100 GHz (Release 14)*, Technical Report 38.811, July 2017. [Online]. Available: https://www.3gpp.org/ftp/Specs/archive/38_series/38.811/38811-d00.zip.

[4] Apple Inc., *Connect to a satellite with your iPhone*, April 2025. [Online]. Available: https://support.apple.com/en-us/105097.

[5] J. M. Gongora-Torres, C. Vargas-Rosales, A. Aragón-Zavala, and R. Villalpando-Hernandez, "Link Budget Analysis for LEO Satellites Based on the Statistics of the Elevation Angle," *IEEE Access*, vol. 10, pp. 14518–14528, 2022.

[6] O. Kodheli *et al.*, "Satellite Communications in the New Space Era: A Survey and Future Challenges," *IEEE Communications Surveys & Tutorials*, vol. 23, no. 1, pp. 70–109, Firstquarter 2021.

[7] 3GPP, *3GPP TS 23.501 version 17.4.0 Release 17*, Technical Specification, September 2021. [Online]. Available: https://www.etsi.org/deliver/etsi_ts/123500_123599/123501/17.04.00_60/ts_123501v170400p.pdf.

[8] 3GPP, *Solutions for NR to support Non-Terrestrial Networks (NTN)*, Technical Report 38.821, version 16.2.0, April 2023. [Online]. Available: https://www.3gpp.org/dynareport/38821.htm.

[9] ITU, *Specific attenuation model for rain for use in prediction methods*, ITU-R Recommendation P.838-3, March 2005. [Online]. Available: https://www.itu.int/dms_pubrec/itu-r/rec/p/r-rec-p.838-3-200503-i!!pdf-e.pdf.

[10] ITU, *Attenuation by atmospheric gases and related effects*, ITU-R Recommendation P.676-12, August 2019. [Online]. Available: https://www.itu.int/dms_pubrec/itu-r/rec/p/R-REC-P.676-12-201908-S!!PDF-E.pdf.

[11] A. Guidotti, A. Vanelli-Coralli, A. Mengali, and S. Cioni, "Non-Terrestrial Networks: Link Budget Analysis," in *Proc. IEEE ICC*, 2020, pp. 1–7.

[12] ESA, *Low Earth orbit*, March 2020. [Online]. Available: `https://www.esa.int/ESA_Multimedia/Images/2020/03/Low_Earth_orbit`.

[13] I. Latachi *et al.*, "Link budget analysis for a LEO CubeSat communication subsystem," in *Proc. IEEE ATSIP*, 2017, pp. 1–6.

[14] S. Chen, S. Sun, and S. Kang, "System integration of terrestrial mobile communication and satellite communication — the trends, challenges and key technologies in B5G and 6G," *China Communications*, vol. 17, no. 12, pp. 156–171, Dec. 2020.

[15] ITU, *Characteristics of precipitation for propagation modelling*, ITU-R Recommendation P.837-7, June 2017. [Online]. Available: `https://www.itu.int/dms_pubrec/itu-r/rec/p/R-REC-P.837-7-201706-I!!PDF-E.pdf`.

[16] 3GPP, *Study on New Radio (NR) to support Non-Terrestrial Networks*, Technical Report 38.811, version 15.1.0, June 2019. [Online]. Available: `https://hscc.csie.ncu.edu.tw/38811.pdf`.

[17] ITU, *Rain height model for prediction methods*, ITU-R Recommendation P.839-4, September 2013. [Online]. Available: `https://www.itu.int/dms_pubrec/itu-r/rec/p/R-REC-P.839-4-201309-I!!PDF-E.pdf`.

[18] SpaceX, *Starlink – Satellite Internet Constellation*. [Online]. Available: `https://www.starlink.com/`.